AD-A121 727 SPACECRAFT CHARGING(U) AIR FORCE INST OF TECH 1/2
WRIGHT-PATTERSON AFB OH SCHOOL OF ENGINEERING
R A PASSOW DEC 78 AFIT/GNE/PH/78-8

UNCLASSIFIED F/G 20/2 NL

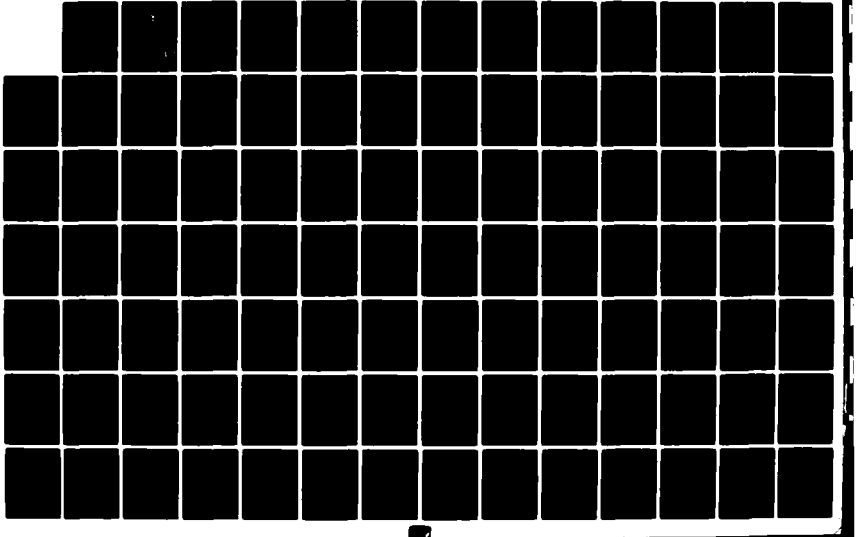

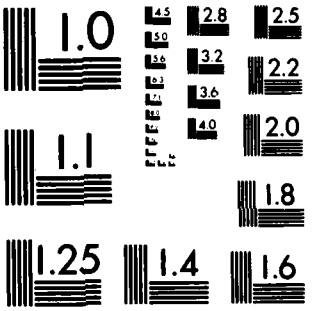

# AIR FORCE INSTITUTE OF TECHNOLOGY

## AIR UNIVERSITY
## UNITED STATES AIR FORCE

SPACECRAFT CHARGING

THESIS

AFIT/GNE/PH/78-8 Richard A. Passow
CPT USA



## SCHOOL OF ENGINEERING



WRIGHT-PATTERSON AIR FORCE BASE, OHIO

AFIT/GNE/PH/78-8

SPACECRAFT CHARGING

Thesis

AFIT/GNE/PH/78-8 Richard A. [illegible]
CPT [illegible]



Approved for public release; distribution unlimited.

AFIT/GNE/PH/78-8

# SPACECRAFT CHARGING

THESIS

Presented to the Faculty of the School of Engineering

Air Force Institute of Technology

Air University

in Partial Fulfillment of the

Requirements for the Degree of

Master of Science




by

Richard A. Passow

CPT US Army

Graduate Nuclear Engineering


December 1978



Approved for public release; distribution unlimited.

## Preface

In March, 1978, the Air Force Weapons Laboratory proposed a thesis topic which involved calculating the electric field inside a spacecraft which had been exposed to a field of incoming current density. This problem interested me for two reasons. First, it has a weapons application, and the results of this project would be useful to the sponsoring office at AFWL. Secondly, working on this type of problem would strengthen my background in electromagnetism.

I would like to express my sincere gratitude to my advisor, Dr. Donn G. Shankland. Without his guidance this project would not have been possible. I would also like to thank Dr. David A. Lee for his assistance with variational calculus, and for his explanation of logarithmic potentials. Special thanks are also due to 1LT Dave Hardin, who helped clarify difficulties encountered with natural boundary conditions, and to Dr. John Jones, who reviewed and critiqued my analytical solution.

Richard A. Passow

## Contents

## Contents

## List of Figures

## List of Symbols

| | |
|---|---|
| $A$ | Represents the area bounded by "S" when used as a limit of integration. |
| $\underline{\underline{A}}$ | Double underline denotes a matrix. |
| $\underline{B}$ | Single underline denotes a column vector. |
| $\delta$ | Represents a delta function or a variance. |
| $\vec{E}$ | Electric field. |
| $g_1, g_2$ | Arbitrary constants. |
| $I$ | Incoming current density. |
| $\vec{J}$ | Current density. |
| $J[\phi]$ | Brackets represent a functional. |
| $\underline{\underline{L}}$ | Lower triangular matrix. |
| $\underline{\underline{Q}}^{\sim}$ | "~" represents the transpose of a matrix. |
| $\phi$ | Potential. |
| $S$ | Represents a functional or an inhomogeneous source term. When used as a limit of integration it represents the boundary of a two-dimensional surface. |
| $\sigma$ | Conductivity. |
| $\sigma_1, \sigma_2$ | Arbitrary constants. |

## Abstract

If a spacecraft is exposed to a steady stream of current density, the charge of which is deposited on the surface of a cylindrical, conducting spacecraft, internal electromagnetic fields are generated. If the internal fields are of sufficient strength, undesirable electronic noise or damage may result. This thesis presents three approaches for calculating the induced $\vec{E}$-Field: separation of variables, variational calculus, and the use of Green's functions.

The spacecraft is modeled as a hollow, infinite cylinder. The fields are calculated for the case in which the incoming current is incident perpendicularly to the longitudinal axis of the cylinder. Basic electro-static theory reveals that the governing equation for the potential is Laplace's Equation, subject to Neumann boundary conditions. This equation is first solved by separation of variables. The $\vec{E}$-Field predicted for representive values of incoming current density are on the order of $10^{-7}$ volts/meter.

Several pitfalls encountered with the variational approach are explained. These include the importance of natural boundary conditions, ensuring continuity of the first derivative across all mesh points, and difficulties encountered in trying to reduce the size of the matrix through "decoupling". The results of this section show that the variational method tends to approximate the analytic solution as the mesh becomes finer.

The Green's function approximations of the potential distribution were consistent with analytic results to at least two significant figures.

# I Introduction

This thesis concerns the calculation of the electric field induced inside a spacecraft (modeled as a cylinder), which has been irradiated by a steady stream of current density. The source of the incoming current is not a factor under consideration. This problem was proposed by the Air Force Weapons Laboratory, and this paper provides an examination of several approaches to the problem's solution.

This project is limited to the study of a non-rotating cylinder which is exposed to a steady stream of current, incident perpendicularly to the cylinder's longitudinal axis. Also, the cylinder is considered to be infinite. This reduces the problem to two dimensions. Thus, the answers calculated will not give the exact fields inside an actual spacecraft. However, the answers are useful as "first cut" approximations to the electric field generated inside a spacecraft. (The fields calculated for a steady stream of incoming current are also valid for the case of an incoming pulse of current, provided it can be assumed that the incoming charge distributes itself around the cylinder very rapidly in comparison to the duration of the pulse.)

Through the use of several simplifying parameters and assumptions, it is shown that the problem reduces to one having a fairly straightforward solution. Thus, the primary emphasis of this thesis will be a comparison of two numerical techniques used to solve the differential equation governing the problem. These two techniques are the use of variational calculus and the use of Green's functions. Initially, the differential equation (Laplace's Equation) and the boundary conditions

are derived. This equation is then solved using separation of variables. The results of this section are used as a basis of comparison with the two other techniques. This is followed by a presentation of the variational approach. First, the appropriate minimization functional is derived. It is then converted to a matrix problem using Simpson's Rule and a three point quadrature formula. The matrix equation is then solved using a Choleski decomposition. The following section contains a discussion of the Green's function method. The Green's function is first derived and then evaluated numerically. The final chapter contains a discussion of the electric field generated using representative values for the dimensions of the cylinder and the magnitude of the incoming current.

The individual chapters contain only the basic logic behind the mathematical techniques and the results of applying them. Detailed derivations of all equations can be found in the appendices. The appendices also contain a discussion of the computer program that was used with each of the three mathematical approaches.

## II Development of a Theoretical Model

### Physical Analysis

The spacecraft is modeled as a non-rotating, hollow, metallic cylinder with a finite conductivity. If this cylinder is irradiated with a uniform, steady stream of current density, charges will be distributed around the cylinder. This distribution of charge will cause a distribution of potential throughout the cylindrical shell, including its inner surface. These potentials, and the resulting current flow, will in turn induce an electric field within the hollow portion of the cylinder. If this electric field is strong enough, undesirable electronic noise or damage may result. Knowledge of the strength of this induced electric field is desirable for obvious military reasons. The procedure for obtaining the electric field is quite straightforward. Once the potential distribution on the inner surface is known, the potential distribution induced in the hollow portion of the cylinder can be calculated. The gradient of this distribution will then give the strength of the electric field within the cylinder.

For a finite cylinder with end caps the current flow throughout the cylindrical shell would have components both parallel and perpendicular to its longitudinal axis. Also, current flow through the end caps would have to be considered. Furthermore, the problem would require a solution in three dimensions. However, by considering an infinite cylinder, the end effects can be neglected, and all current flow will be perpendicular to the longitudinal axis of the cylinder. This simplification reduces the problem to a manageable two-dimensional form.

The electric field predicted by this infinite cylinder model will approximate the electric field near the plane z = height/2 of a finite cylinder.

The two-dimensional form of the problem is illustrated in Fig 2-1. The incoming current density is incident perpendicularly to the longitudinal axis of the cylinder over the interval $-\pi/2 \leq \theta \leq \pi/2$. As the incoming current continues, charge will continue to build up on the outside of the cylinder. It is assumed that this charge has no effect on the incoming beam. The radially outward "leakage" current functions to make the boundary conditions consistent with the mathematics. It is discussed in the section explaining the boundary conditions.

Method of Solution

The current through an arbitrary surface is

$$\int_S \vec{J} \cdot \vec{ds} \tag{2-1}$$

For a closed surface this integral must equal the rate of decrease of charge within it. With the charge designated as q, the result may be written

$$\int_S \vec{J} \cdot \vec{ds} = -\frac{\partial q}{\partial t} \tag{2-2}$$

Through application of the divergence theorem, this surface integral can be changed to a volume integral. Also, when the charge is represented as a volume integral of charge density, $\rho$, Eqn (2-2) can be written

$$\int_V (\nabla \cdot \vec{J})\, dV = -\frac{\partial}{\partial t}\int_V \rho\, dV = -\int_V \frac{\partial \rho}{\partial t}\, dV \tag{2-3}$$

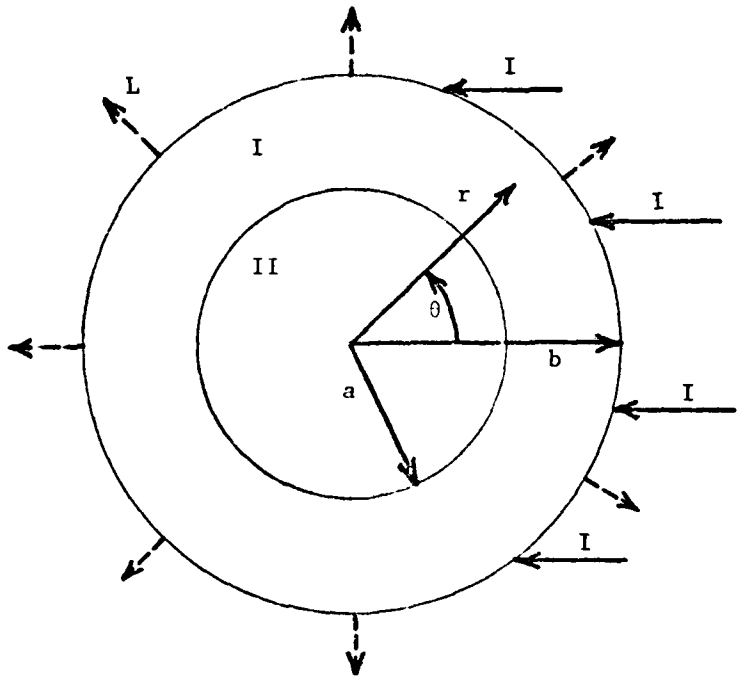


| | | |
|---|---|---|
| ⟵ | = | Incoming Current, I $(-\frac{\pi}{2} \leq \theta \leq \frac{\pi}{2})$ |
| <----- | = | Leakage Current, L $(0 \leq \theta \leq 2\pi)$ |
| a | = | Inner Radius |
| b | = | Outer Radius |
| r | = | Arbitrary Radial Distance |
| θ | = | Arbitrary Angular Displacement |
| I | = | Metallic Region Through which Current Flows |
| II | = | Region in which the Induced Fields are Desired |

Fig 2-1. Schematic Drawing of the Theoretical Model.

Since the surface is constant, the partial derivative with respect to time can be brought inside the integral. Equating integrands yields the continuity equation

$$\nabla \cdot \vec{J} = -\frac{\partial \rho}{\partial t} \tag{2-4}$$

For the steady state condition $\frac{\partial \rho}{\partial t} = 0$. For an isotropic medium (both regions I and II are considered to be isotropic), $\vec{J} = \sigma\vec{E}$. Thus

$$\nabla \cdot \sigma\vec{E} = 0 \tag{2-5}$$

Replacing E with $-\nabla\phi$ yields Laplace's Equation

$$\nabla^2\phi = 0 \tag{2-6}$$

This equation is valid for both regions of the cylinder. Thus, Laplace's Equation, subject to appropriate boundary conditions, must first be solved for Region I. This will yield the potential on the inner boundary. Then Laplace's Equation is solved for Region II, subject to the previously calculated values of $\phi$ at the inner boundary. This gives the values of $\phi$ throughout Region II. The strength of the $\vec{E}$ field in this region can then be determined from $\vec{E} = -\nabla\phi$.

Boundary Conditions

Current density, the electric field, and potential are related by

$$\vec{J} = \sigma\vec{E} = -\sigma\vec{\nabla}\vec{\phi} \tag{2-7}$$

or

$$\vec{\nabla}\vec{\phi} = -\frac{\vec{J}}{\sigma} \tag{2-8}$$

On the outer boundary, only the normal component of the incoming

current, I, is known. The tangential component cannot be specified because the current flow around the cylinder is unknown.

On the inner boundary the normal component of $\nabla\phi$ (i.e. the current) is zero. This is because the inside wall is not being irradiated, and all current flow at the inner boundary is tangential to the boundary. There is no current flow from Region I of the cylinder, across the inner boundary, into Region II. As before, the tangential component of $\nabla\phi$ cannot be specified because the current flow is unknown.

Thus, the apparent boundary conditions are, for the outer boundary,

$$\frac{\partial\phi}{\partial n} = \frac{\partial\phi}{\partial\tau} = \begin{cases} -\left(\dfrac{-I\cos\theta}{\sigma}\right) & -\dfrac{\pi}{2} \le \theta \le \dfrac{\pi}{2} \\ 0 & \dfrac{\pi}{2} \le \theta \le \dfrac{3\pi}{2} \end{cases} \tag{2-9}$$

and for the inner boundary

$$\frac{\partial\phi}{\partial n} = \frac{\partial\phi}{\partial\tau} = 0 \qquad 0 \le \theta \le 2\pi \tag{2-10}$$

However, the divergence theorem states

$$\int_A \nabla^2\phi \, dA = \oint_S \frac{\partial\phi}{\partial n} \, ds \tag{2-11}$$

Since $\nabla^2\phi = 0$, it is obvious that

$$\oint_S \frac{\partial\phi}{\partial n} \, ds = 0 \tag{2-12}$$

However, integrating around both boundaries with the boundary conditions as specified in Eqns (2-9) and (2-10) yields

$$\int_{S_{inner}} \frac{\partial \phi}{\partial r}\, ds + \int_{S_{outer}} \frac{\partial \phi}{\partial r}\, ds \stackrel{?}{=} 0 \tag{2-13}$$

$$0 + b\int_{-\frac{\pi}{2}}^{\frac{\pi}{2}} \frac{I\cos\theta}{\sigma}\, d\theta \stackrel{?}{=} 0 \tag{2-14}$$

$$\frac{2bI}{\sigma} \neq 0 \tag{2-15}$$

Thus, the boundary conditions as stated in Eqns (2-9) and (2-10) must be modified to satisfy the divergence theorem. This modification consists of adding a radially outward "leakage current" on to the outer boundary. Its value is taken to be constant over the outer boundary, as shown in Fig 2-1. With the addition of this term the outer boundary condition becomes

$$\frac{\partial \phi}{\partial r} = \begin{cases} -\left(\frac{-I\cos\theta + L}{\sigma}\right) & -\frac{\pi}{2} \leq \theta \leq \frac{\pi}{2} \\ -\frac{L}{\sigma} & \frac{\pi}{2} \leq \theta \leq \frac{3\pi}{2} \end{cases} \tag{2-16}$$

where L is a value such that

$$b\int_0^{2\pi} \frac{\partial \phi}{\partial r}\, d\theta = 0 \tag{2-17}$$

When the values for $\frac{\partial \phi}{\partial r}$ are substituted over the appropriate angular regions, Eqn (2-12) becomes

$$b\int_{-\frac{\pi}{2}}^{\frac{\pi}{2}}\left(\frac{I\cos\theta - L}{\sigma}\right)d\theta + b\int_{\frac{\pi}{2}}^{\frac{3\pi}{2}} -\frac{L}{\sigma}\,d\theta = 0 \qquad (2\text{-}18)$$

Simplifying and evaluating the integrals yields

$$-I\sin\theta\Big|_{-\frac{\pi}{2}}^{\frac{\pi}{2}} - L\theta\Big|_{0}^{2\pi} = 0 \qquad (2\text{-}19)$$

From which

$$L = -\frac{I}{\pi} \qquad (2\text{-}20)$$

Thus, the differential equation and boundary conditions are,

$$\nabla^2\phi = 0 \qquad (2\text{-}21)$$

$$\left.\frac{\partial\phi}{\partial r}\right|_{r=a} = 0$$

$$\left.\frac{\partial\phi}{\partial r}\right|_{r=b} = \begin{cases} \frac{I}{\sigma}\left(\cos\theta - \frac{1}{\pi}\right) & -\frac{\pi}{2} \le \theta \le \frac{\pi}{2} \\ -\frac{I}{\sigma\pi} & \frac{\pi}{2} \le \theta \le \frac{3\pi}{2} \end{cases}$$

## III Solution by Separation of Variables

### Solution in Region I

Through application of the method of separation of variables, the general solution for Laplace's Equation, subject to the boundary conditions as listed in Eqn (2-21), is

$$\phi_I(r,\theta) = \frac{I b^2 \cos\theta}{2\sigma(b^2 - a^2)}\left(r + \frac{a^2}{r}\right) + \sum_{n=1}^{\infty} \frac{(-1)^{n-1} I b^{2n+1} \cos(2n\theta)}{n\sigma\pi(4n^2-1)(b^{4n} - a^{4n})}\left(r^{2n} + \frac{a^{4n}}{r^{2n}}\right) \qquad (3\text{-}1)$$

This equation gives the potential distribution throughout Region I. A detailed derivation of Eqn (3-1) can be found in Appendix A. Appendix B contains the Fourier expansion of the boundary conditions.

### Solution in Region II

Laplace's Equation must also be solved for the potentials throughout Region II, subject to Dirichlet boundary conditions because the potentials on the inner boundary are now known. The boundary condition for Region II is

$$\phi_{II}(a,\theta) = f(a,\theta) \qquad (3\text{-}2)$$

where $f(a,\theta)$ is given by the solution to Region I at r=a.

The solution of Laplace's Equation, subject to the boundary condition as given in Eqn (3-2), for Region II is

$$\Phi_{II}(r,\theta) = \frac{I b^2 r \cos\theta}{\sigma(b^2 - a^2)} + \sum_{n=1}^{\infty} \frac{(-1)^{n-1} 2 I b^{2n+1} r^{2n} \cos(2n\theta)}{n\pi\sigma(4n^2-1)(b^{4n} - a^{4n})} \qquad (3\text{-}3)$$

This equation is derived in Appendix A.

$\vec{E}$-Field in Region II

Since $\vec{E} = -\nabla\phi$, and the gradient of $\phi$ in cylindrical coordinates is

$$\nabla\phi = \frac{\partial\phi}{\partial r}\hat{r} + \frac{1}{r}\frac{\partial\phi}{\partial\theta}\hat{\theta} \qquad (3\text{-}4)$$

the $\vec{E}$-field given by the potential distribution in Eqn (3-3) is

$$\vec{E} = \left[-\frac{I b^2 \cos\theta}{\sigma(b^2 - a^2)} - \sum_{n=1}^{\infty} \frac{(-1)^{n-1} 4 I b^{2n+1} r^{2n-1} \cos(2n\theta)}{\sigma\pi(4n^2-1)(b^{4n} - a^{4n})}\right]\hat{r}$$

$$+ \left[-\frac{I b^2(-\sin\theta)}{\sigma(b^2 - a^2)} - \sum \frac{(-1)^{n-1} 4 I b^{2n+1} r^{2n-1} (-\sin 2n\theta)}{\sigma\pi(4n^2-1)(b^{4n} - a^{4n})}\right]\hat{\theta} \qquad (3\text{-}5)$$

Appendix C contains a computer program based on Eqn (3-5) which calculates the magnitude of the $\vec{E}$-field for an arbitrary r and $\theta$, using

$$|\vec{E}| = \sqrt{(a_r)^2 + (a_\theta)^2} \qquad (3\text{-}6)$$

Test Solution in Region I

The solutions given in the previous paragraphs represent solutions for the problem as derived in Chapter II. However, to aid in the comparison of the results of the two other techniques, a simpler outer boundary condition was used. This condition is

$$\left.\frac{\partial\phi}{\partial r}\right|_{r=b} = \cos\theta \qquad 0 \le \theta \le 2\pi \qquad (3\text{-}7)$$

This condition has the advantage of reducing the Fourier expansion of $f(\theta)$ to only one term.

The solution to Laplace's Equation, subject to the above outer boundary condition is

$$\phi(r,\theta) = \frac{b^2}{(b^2-a^2)}\left(r + \frac{a^2}{r}\right)\cos\theta \qquad (3\text{-}8)$$

For ease of calculation, the inner and outer radii will be 2 and 4 respectively. Substitution of these values yields

$$\phi(r,\theta) = \frac{4}{3}\left(r + \frac{4}{r}\right)\cos\theta \qquad (3\text{-}9)$$

which will be used to compare the accuracy of the results of the variational and Green's function approaches.

## IV Variational Calculus Approach

### Solution Procedure

The principle behind the variational approach is that of minimizing a functional. For the problem as outlined in Chapter I the functional, S, is

$$S = \frac{1}{2}\int_A (\nabla\phi)^2 \, dA + \frac{1}{2}\int_\theta -2\phi f(\theta) r \, d\theta \qquad (4\text{-}1)$$

where the second integral is over the outer boundary, and $f(\theta)$ is the outer boundary condition. There is no integral term for the inner boundary because $f(\theta) = 0$ on the inner boundary. This functional is derived in Appendix D.

Through the use of a 3-point quadrature formula and Simpson's Rule, Eqn (4-1) can be written in matrix form as

$$S = \frac{1}{2}\tilde{\Phi}\,\underline{\underline{A}}\,\underline{\Phi} - \tilde{\Phi}\,\underline{\underline{B}}\,f(\theta)\underline{b} \qquad (4\text{-}2)$$

where $\underline{\underline{A}}$ is the coefficient matrix resulting from application of Simpson's Rule and the quadrature formula, and $\underline{B}$ is a column vector containing the Simpson's Rule coefficients for the mesh points on the outer boundary.

Taking the variance of S with respect to $\underline{\phi}$ yields

$$\frac{\delta S}{\delta \tilde{\Phi}} = \underline{\underline{A}}\,\underline{\Phi} - \underline{\underline{B}}\,f(\theta)\underline{b} \qquad (4\text{-}3)$$

Since S is to be minimized, the variance must be zero, so

$$\underline{\underline{A}}\,\underline{\Phi} - \underline{\underline{B}}\,f(\theta)\underline{b} = 0 \qquad (4\text{-}4)$$

Thus, the matrix equation is

$$\underline{\underline{A}}\,\underline{\phi} = \underline{\underline{B}}\,f(\theta)\,\underline{b} \tag{4-5}$$

Equation (4-5) can be written in the form

$$\underline{\underline{L}}\,\underline{\underline{\tilde{L}}}\,\underline{\phi} = \underline{Y} \tag{4-6}$$

where $\underline{\underline{L}}$ is a lower triangular Choleski decomposition of $\underline{\underline{A}}$.

Equation (4-6) can be easily solved by letting

$$\underline{\underline{L}}\,\underline{x} = \underline{Y} \tag{4-7}$$

and solving for $\underline{x}$ using forward substitution. Once $\underline{x}$ is known, $\phi$ can be calculated using backward substitution.

Since the original problem contains Neumann boundary conditions, it is only possible to specify $\phi$ to within an additive constant. This is manifested in the fact that the coefficient matrix, $\underline{\underline{A}}$, will be singular. When $\underline{\underline{A}}$ is decomposed via a Choleski decomposition, the lower right term in the main diagonal of $\underline{\underline{L}}$ will be zero. Thus, the last term in each of the $\underline{x}$, $\underline{y}$, and $\underline{\phi}$ vectors cannot be solved for directly, because that would entail dividing by zero. This difficulty can be alleviated by only solving for the first N-1 terms in each vector, and arbitrarily setting the Nth term equal to zero. The solution so calculated will be correct within an additive constant. To arrive at the minimum solution, (one which is orthogonal to $\underline{\tilde{e}} = (1,1,1,\ldots 1)$, the zero eigenvalue-eigenvector of $\underline{\underline{A}}$), it will be necessary to normalize the solution. That is, total all the terms, find the average, and subtract this average from each term in the solution vector. A computer program for the variational approach is listed and discussed in Appendix G.

Matrix Form of the Double Integral

The first integral in Eqn. (4-1) can be converted to a double integral over r and θ, using the relation dA = rdrdθ. The integral is then expressed as a double sum.

$$\frac{1}{2}\int_A (\nabla\phi)^2 dA = \frac{1}{2}\int_\theta \int_r r(\nabla\phi)^2 dr\, d\theta \tag{4-8}$$

$$= \frac{1}{2}\sum_i \sum_j A_i A_j r_j (\nabla\phi)^2_{ij} \Delta r \Delta\theta \tag{4-9}$$

where $A_i$ and $A_j$ are Simpson's Rule coefficients.

Since

$$(\nabla\phi)^2 = \left(\frac{\partial\phi}{\partial r}\right)^2 + \frac{1}{r^2}\left(\frac{\partial\phi}{\partial\theta}\right)^2 \tag{4-10}$$

it will be necessary to have difference relations for both r and θ. Also, since each difference relation will have to be squared, it will be advantageous to use ones which don't have too many terms, yet are reasonably accurate. The following 3-point formula are accurate to order $h^2$ (Ref: 8, 96).

$$\frac{\partial\phi}{\partial r} = \frac{1}{2\Delta r}\left(-3\phi_{0,j} + 4\phi_{1,j} - \phi_{2,j}\right) \tag{4-11a}$$

$$\frac{\partial\phi}{\partial r} = \frac{1}{2\Delta r}\left(-\phi_{i-1,j} + \phi_{i+1,j}\right) \tag{4-11b}$$

$$\frac{\partial\phi}{\partial r} = \frac{1}{2\Delta r}\left(\phi_{N-2,j} - 4\phi_{N-1,j} + 3\phi_{N,j}\right) \tag{4-11c}$$

Eqn (4-11a) is used for all mesh points on the inner boundary, and Eqn (4-11c) is used for all mesh points on the outer boundary. However, care must be used when approximating the derivative at the interior mesh points.

Initially, Eqn (4-11b) was used to approximate the derivative at all interior mesh points. However, this produced the scalloping phenomena shown in Fig 4-1. No matter how fine a mesh was used, the scalloping was always present, and always over 3-point segments. The reason the scallops are present can be explained by the following analysis:

If the boundary term is ignored, the functional has the form (in one dimension)

$$S = \frac{1}{2}\int_a^b (\phi')^2 \, dr \tag{4-12}$$

The variance of S with respect to $\phi'$ is

$$\delta S = \int_a^b (\delta\phi')\,\phi' \, dr \tag{4-13}$$

If S is a minimum, $\delta S = 0$. Also, if the curve (a,b) is approximated by two piecewise continuous functions in the intervals, $(a,c^-)$ and $(c^+,b)$, Eqn (4-13) can be written

$$\int_a^{c^-} (\delta\phi')\,\phi' \, dr + \int_{c^+}^b (\delta\phi')\,\phi' \, dr = 0 \tag{4-14}$$

If both integrals are integrated by parts, this equation becomes

$$\delta\phi\phi'\Big|_a^{c^-} + \delta\phi\phi'\Big|_{c^+}^{b} - \int_a^{c^-}\delta\phi\phi''dr - \int_{c^+}^{b}\delta\phi\phi''dr = 0 \qquad (4\text{-}15)$$

Evaluating the first two terms and combining the integrals yields

$$\delta\phi_a\phi'_a - \delta\phi_{c^-}\phi'_{c^-} + \delta\phi_{c^+}\phi'_{c^+} - \delta\phi_b\phi'_b - \int_a^b\delta\phi\phi'' = 0 \qquad (4\text{-}16)$$

Due to the boundary conditions, the terms evaluated at "a" and "b" are both zero. Also, since the function in the interval from a to c to b is continuous, Eqn (4-16) can be written

$$\delta\phi_c\left(\phi'_{c^+} - \phi'_{c^-}\right) = \int_a^b\delta\phi\phi'' \qquad (4\text{-}17)$$

Thus, since continuity of the first derivative is not enforced across each segment, the functional has been given the freedom to absorb some of the "cost" of minimization by letting the slope be discontinuous across each piecewise continuous segment. The reason the scallops occurred in groups of three points is because both Simpson's Rule and a 3-point quadrature formula were used in the numerical approximation, implying a quadratic function over a 3-point range.

To eliminate the scalloping, Eqns (4-11a) and (4-11c) were used to approximate both the left and right derivatives at the mesh points which are junctions for each of the 3-point segments (e.g., mesh point $\phi_{i,j}$ in Fig E-1). This procedure more accurately calculates the actual value of

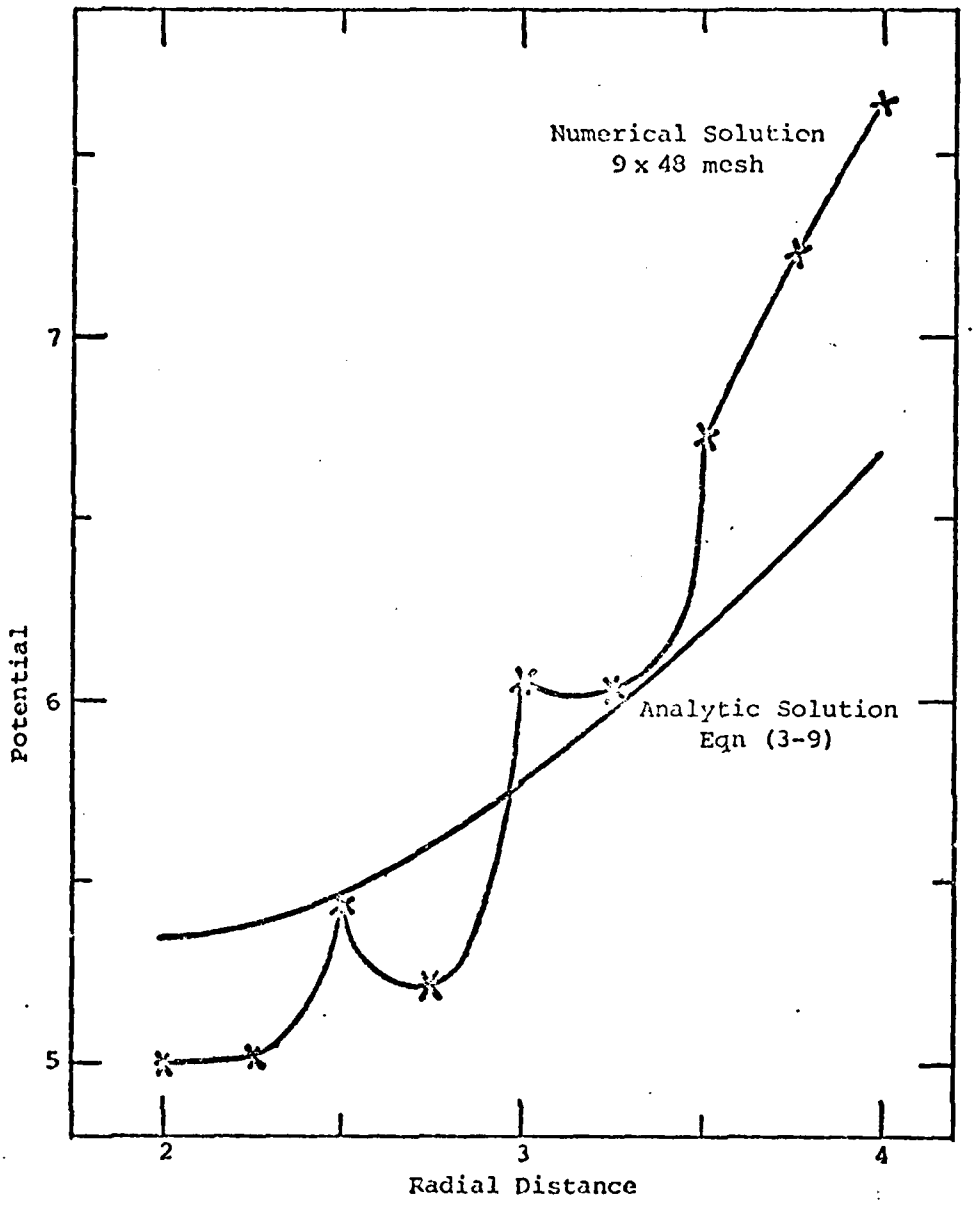


Fig 4-1. Scalloping Phenomena When Continuity of the 1st Derivative Is Not Enforced Across All Mesh Points.

the derivative on either side of the break-point, so that large slopes (scalloping) will be suppressed.

Eqn (4-11b) can be used to approximate the derivative at the middle mesh point of each 3-point segment. In this case continuity is enforced through the use of Simpson's Rule. Use of the approximation formulae in this manner produced a smooth curve for the approximation in the radial direction.

Similarly, care must be used when approximating the angular derivatives of Eqn (4-10). Initially, angular derivatives at all mesh points were approximated with Eqn (4-11b). As can be seen in Fig 4-2, the results of this approximation bracket, but never approach, the analytic answer. The values along the even numbered radials are always greater, and the values along the odd numbered radials are always less than the analytic answer. Again, this results from an improper approximation of the first derivative in the angular direction. This was corrected by using Eqns (4-11a) and (4-11b) to approximate the left and right angular derivatives at all mesh points. Again, an additional factor of $\frac{1}{2}$ was included in both Eqns (4-11a) and (4-11b) to account for the use of both left and right derivatives. Use of the approximation formulae in this manner produced a smooth curve for the approximation in the angular direction.

Matrix Form of the Single Integral

The second integral in Eqn (4-1) can be converted into the following summation:

$$\frac{1}{2}\int_{\theta} -2 f(\theta) r \, d\theta = -\sum_{i} B_i f(\theta)_i \, b \, \Delta\theta \qquad (4\text{-}18)$$

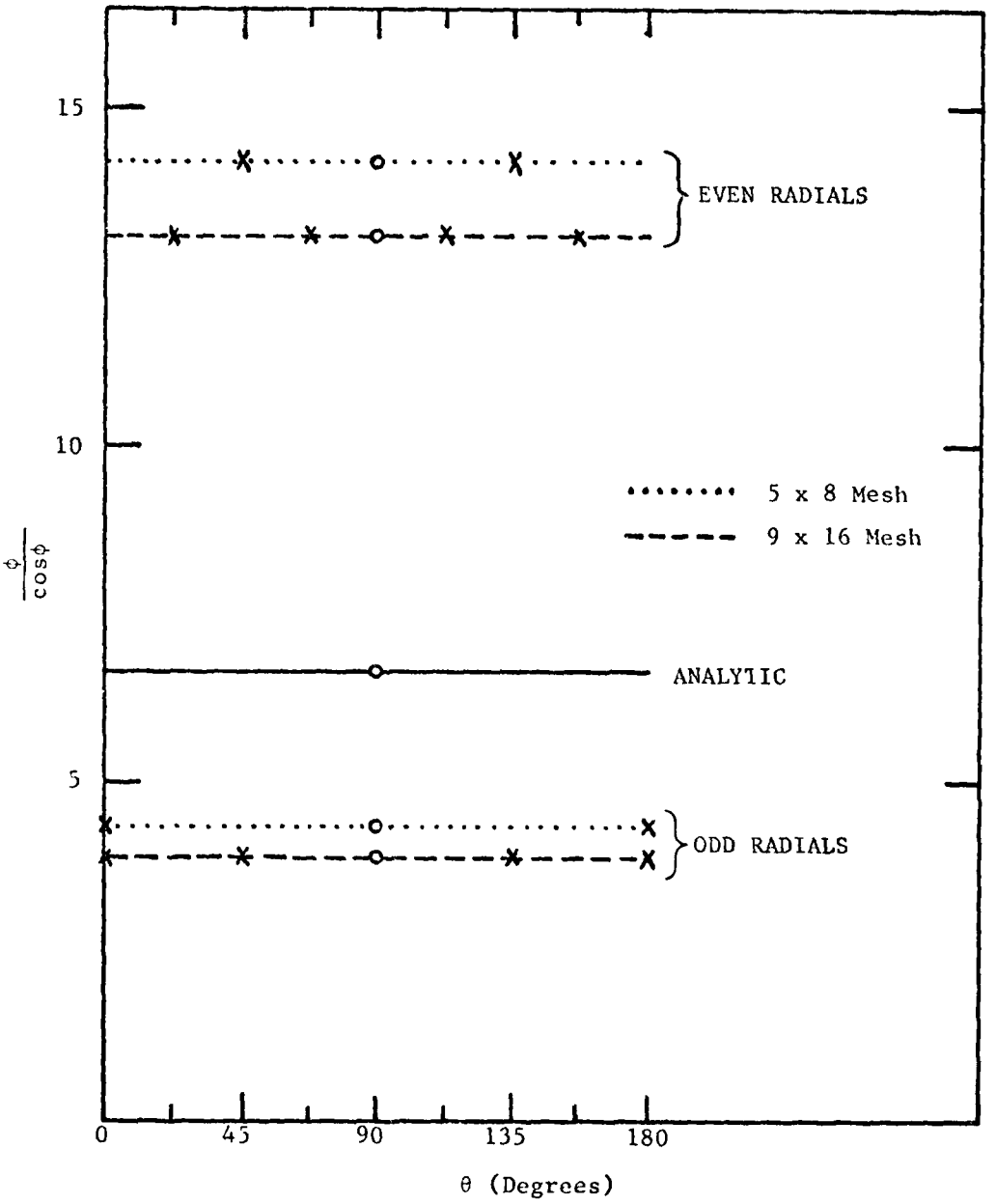


Fig 4-2. Plot of $\phi/\cos\phi$ vs theta along the outer boundary. Continuity of the first derivative in the angular direction is not enforced.

No difference formulae are needed because there are no derivatives to approximate. In fact, the only non-zero terms in the left hand side vector will be those terms corresponding to a value of $\phi$ on the outer boundary.

Summary

Initially, the boundary conditions were enforced with Lagrange Multipliers, without considering the natural boundary conditions of the functional. This produced a scalloped curve with endpoints at or near zero. (This initial attempt is discussed in Appendix F.) When the natural boundary conditions were included in the functional, the curve was "pulled up" so that its endpoints more closely approximated the analytic values. However, the scallops were still present no matter how fine a mesh was used. These scallops were present because continuity of the first derivative was not rigidly enforced in the numerical approximation. When both left and right radial derivatives of the mesh points which were junctions of the 3-point segment were used, the numerical solution did indeed become a smooth curve. However, it still did not satisfactorily approximate the analytic solution. Finally, both left and right derivatives in the angular direction were approximated for all mesh points. As illustrated in Fig. 4-3, the numerical solution approaches the analytic result as the mesh becomes finer. However, for a 9 x 32 mesh it was necessary to use 168 K of computer storage.

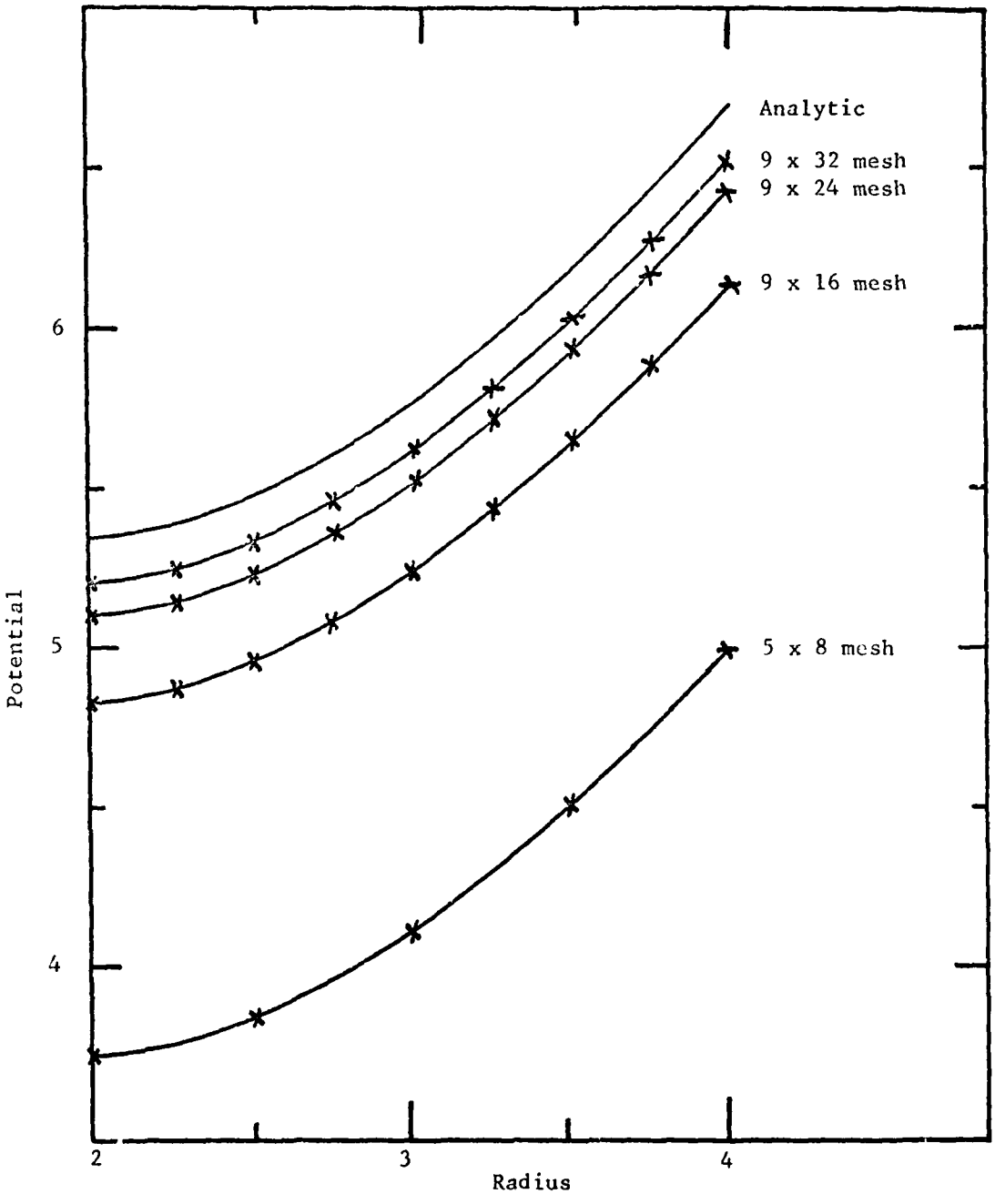


Fig 4-3. Comparison of the Analytic Solution with the Variational Solution Along the Line $\theta = 0$.

## V Solution Using Green's Functions

In this chapter the equations developed in Chapter 1 are solved using a Green's function. First, a solution for $\phi$ is derived in terms of a Green's function. Second, an iterative scheme for obtaining the values of $\phi$ is presented.

### Reduction to Integral Equation

The basic equation is

$$\nabla^2 \phi = 0 \tag{5-1}$$

with boundary conditions

$$\left.\frac{\partial \phi}{\partial r}\right|_{r=a} = 0$$

$$\left.\frac{\partial \phi}{\partial r}\right|_{r=b} = f(\phi)$$

The Green's function expression for Eqn (5-1) is

$$\nabla^2 G(\vec{x}, \vec{x}') = \delta(\vec{x}-\vec{x}') \tag{5-2}$$

where $\vec{x}$ is the observer's point and $\vec{x}'$ is the source point, as measured from the origin. Since the Green's function only depends on the difference between the two vectors, $\vec{x}$ and $\vec{x}'$, it can be written as $G(\vec{x}-\vec{x}')$.

Multiplying Eqn (5-1) by $G(\vec{x}-\vec{x}')$ and Eqn (5-2) by $\phi(\vec{x})$ yields

$$G(\vec{x}-\vec{x}')\nabla^2\phi(\vec{x}) = 0 \tag{5-3}$$

and

$$\phi(\vec{x})\nabla^2 G(\vec{x}-\vec{x}') = \delta(\vec{x}-\vec{x}')\,\phi(\vec{x}) \tag{5-4}$$

Subtracting Eqn (5-3) from Eqn (5-4), and integrating over the volume of the cylinder results in

$$\int_V \left[-G(\vec{x}-\vec{x}')\nabla^2\phi(\vec{x}) + \phi(\vec{x})\nabla^2 G(\vec{x}-\vec{x}')\right] dV = \phi(\vec{x}') \quad (5\text{-}5)$$

If one of the "del" terms is factored out of the brackets, the volume integral can be converted to a surface integral through application of the divergence theorem.

$$\int_A \left[\phi(\vec{x})\nabla G(\vec{x}-\vec{x}') - G(\vec{x}-\vec{x}')\nabla\phi(\vec{x})\right]\cdot da' = \phi(\vec{x}') \quad (5\text{-}6)$$

Since the Green's function is symmetric, the observer's point, $\vec{x}$, and the source point, $\vec{x}'$, can be interchanged. This change results in

$$\phi(\vec{x}) = \int_A \left[\phi(\vec{x}')\nabla' G(\vec{x}'-\vec{x}) - G(\vec{x}'-\vec{x})\nabla'\phi(\vec{x}')\right]\cdot da' \quad (5\text{-}7)$$

If a new function, $\Psi(\vec{x})$, is defined as

$$\Psi(\vec{x}) = -\int_A G(\vec{x}'-\vec{x})\nabla'\phi(\vec{x}')\cdot da' \quad (5\text{-}8)$$

Eqn (5-7) can be written as

$$\phi(\vec{x}) = \Psi(\vec{x}) + \int_A \phi(\vec{x}')\nabla' G(\vec{x}'-\vec{x})\cdot da' \quad (5\text{-}9)$$

Equations (5-8) and (5-9) can be solved by iteration, viz.,

$$\phi_0(\vec{x}) = \Psi(\vec{x}) \quad (5\text{-}10a)$$

$$\phi_n(\vec{x}) = \Psi(\vec{x}) + \int_A \phi_{n-1}(\vec{x})\nabla' G(\vec{x}'-\vec{x})\cdot da' \quad (5\text{-}10b)$$

where

$$G(\vec{x}' - \vec{x}) = \frac{\ln |\vec{x}' - \vec{x}|}{\pi} \tag{5-11}$$

and

$$\nabla' G(\vec{x}' - \vec{x}) = \frac{\vec{x}' - \vec{x}}{\pi |\vec{x}' - \vec{x}|^2} \tag{5-12}$$

Eqns (5-11) and (5-12) are derived in Appendix H. Also, a more rigorous derivation of the integral equation, Eqn (5-7) can be found in Appendix I.

The iteration scheme is explained in the following six steps.

1. The cylindrical shell is divided into an even number of equally spaced angular intervals. Since Eqns (5-8) and (5-9) only contain surface integrals, there is no need for interior mesh points. (This is one advantage of using Green's functions - the number of mesh points can be drastically reduced, thus saving computer storage space.)

2. Equation (5-8) is used to calculate the value of $\psi(\vec{x})$ for each mesh point on the inner boundary due to contributions from every mesh point on the outer boundary.

3. Equation (5-8) is used to calculate the value of $\psi(\vec{x})$ for each mesh point on the outer boundary due to contributions from every mesh point on the outer boundary.

Note: In both steps 2 and 3 there is no contribution from the inner boundary because $\nabla\phi \cdot da = \partial\phi/\partial r = 0$ on the inner boundary.

4. Equation (5-9) is used to calculate the value of $\phi$ for every mesh point on the inner boundary due to contributions from all mesh points on both boundaries. The corresponding value of $\psi$ is then added to the sum of these contributions.

5. Step 4 is repeated for all mesh points on the outer boundary.

6. Steps 4 and 5 are repeated until all values of $\phi$ converge to within some tolerance limit.

A computer program implementing the above iteration scheme can be found in Appendix J.

The values of $\phi$ calculated by this method are in agreement to three significant figures with the values predicted by the test solution of Eqn (3-9). In this calculation, 128 mesh points were used around each boundary and the values of the conductivity and incoming current were set to unity. The computer program was then modified to accommodate the boundary conditions as listed in Eqn (2-21). Once again, the values of $\phi$ were in agreement to three significant figures. A comparison of the results was not plotted because the curves would be indistinguishable.

Solution in Region II

The procedure is the same as that used in the previous section up to Eqn (5-7). On the inner boundary $\nabla\phi(\vec{x}') = 0$, so Eqn (5-7) can be written

$$\phi(\vec{x}) = \int_A \nabla' G(\vec{x}' - \vec{x})\, \phi(\vec{x}') \cdot da' \qquad (5\text{-}13)$$

where $\nabla' G(\vec{x}' - \vec{x})$ is given in Eqn (5-12) and the values of $\phi(\vec{x}')$ have been calculated by the method presented in the previous section.

Thus, it is not necessary to iterate a solution, just sum the contributions from all points on the inner boundary. The summation expression for Eqn (5-13) is

$$\phi(\vec{x}') = \frac{a\Delta\theta}{\pi} \sum_{n=1}^{N} \frac{\cos\gamma_n\, \phi(\theta)_n}{|\vec{x}' - \vec{x}|_n} \qquad (5\text{-}14)$$

where $\gamma$ is the angle between $\vec{x}' - \vec{x}$ and the outward unit normal at x'.

The potentials obtained with this formula are in agreement to two significant figures with the values predicted by Eqn (3-3).

Calculation of the $\vec{E}$-Field

It is not necessary to calculate the values of $\Phi$ throughout region II. Eqn (5-13) can be used to calculate the electric field directly. Since $\vec{E} = -\nabla\phi$, Eqn (5-13) can be written (after the dot product operation is performed)

$$-\nabla\phi(\vec{x}) = -\nabla\int_S \frac{\partial}{\partial n} G(\vec{x}' - \vec{x})\,\phi(\vec{x}')\,ds \qquad (5\text{-}15)$$

The gradient operation is with respect to $\vec{x}$, not $\vec{x}'$, so Eqn (5-15) becomes

$$\vec{E} = -\int_S \phi(\vec{x}')\left[\frac{\partial}{\partial r}\left(\frac{\partial G}{\partial n}\right)\hat{r} + \frac{1}{r}\frac{\partial}{\partial\theta}\left(\frac{\partial G}{\partial n}\right)\hat{\theta}\right]ds \qquad (5\text{-}16)$$

Summary

The Green's function method approximated the values of $\phi$ as predicted by the analytical formulas of Chapter III to at least two significant figures. Thus, the Green's function method gave an independent verification of Eqns (3-1) and (3-3). Time did not permit a computer implementation of Eqn (5-16).

## VI Representative Values of the Magnitude of the $\vec{E}$-Field

In this chapter the electric field induced inside the hollow portion of the cylinder is calculated using Eqns (3-5) and (3-6). The following representative values are used for the input parameters:

Outer radius: .5 meters

Cylinder thickness: varied from .254 to 2.54 millimeters (10 to 100 mils)

Conductivity (Aluminum): $3.82 \times 10^7$ mhos/meter

Incoming current density: .01 amps/meter$^2$

Fig 6-1 illustrates how the maximum strength of the electric field varies with the thickness of the cylinder.

Fig 6-2 illustrates the magnitude of the electric field as it varies with angle. Each curve plots the field along an equi-radial arc. Since the electric field is symmetric with respect to the line $\theta = 0$, only the fields in the upper half of the cylinder are plotted. As can be seen from the figure, the maximum value of the $\vec{E}$-Field occurs at the inner boundary when $\theta = 0$.

Both figures indicate that for an incoming current density of .01 amps/meter$^2$, the strength of the electric field inside the cylinder is on the order of $10^{-7}$ volts/meter. Eqn (3-5) indicates that the magnitude of the electric field varies directly as the incoming current. Thus, to start getting appreciable fields inside the cylinder, the incoming current density would have to be on the order of $10^5$-$10^6$ amps/meter$^2$.

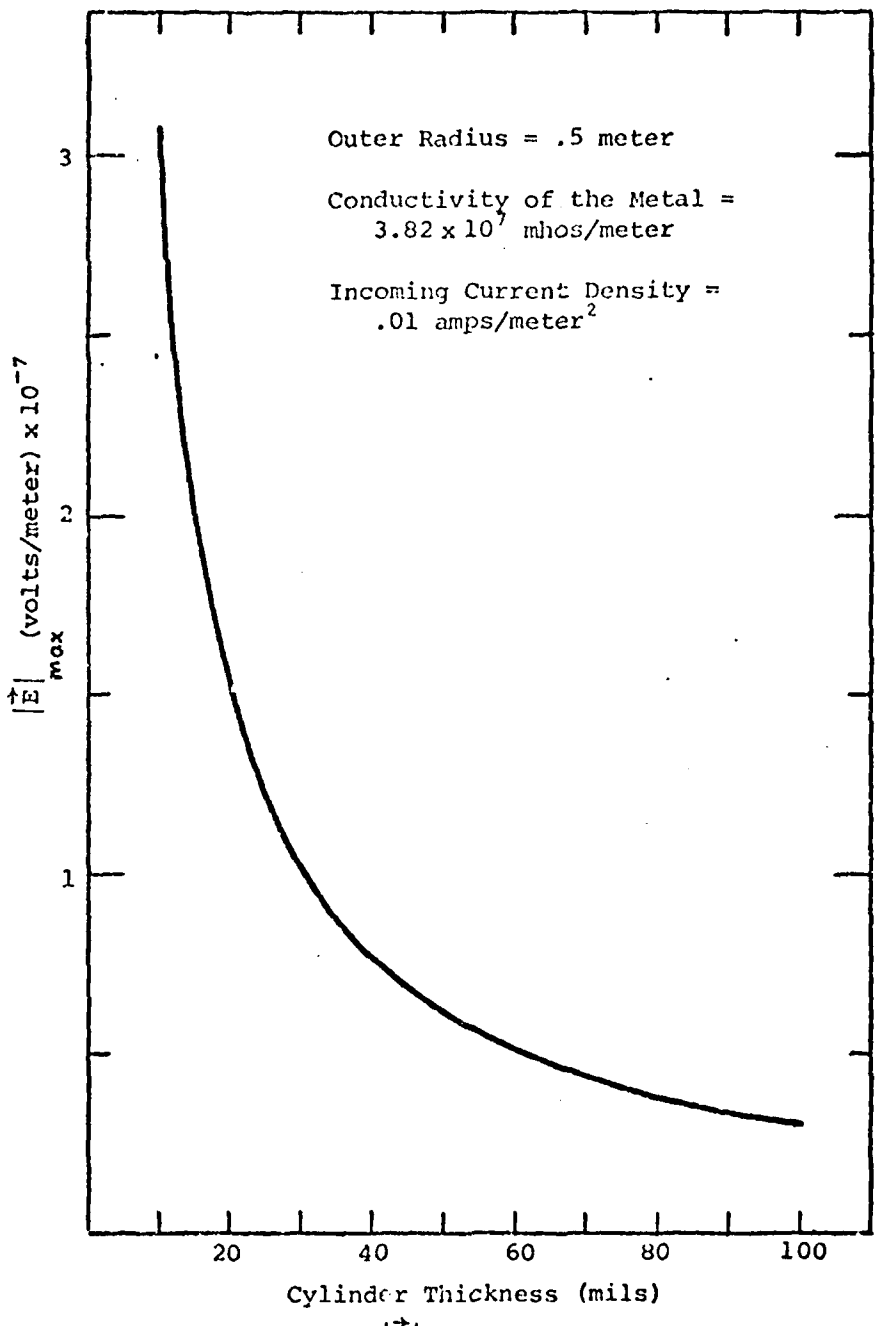


Fig 6-1. Plot of $|\vec{E}|_{max}$ vs Cylinder Thickness for an Aluminum Cylinder with a Radius of .5m.

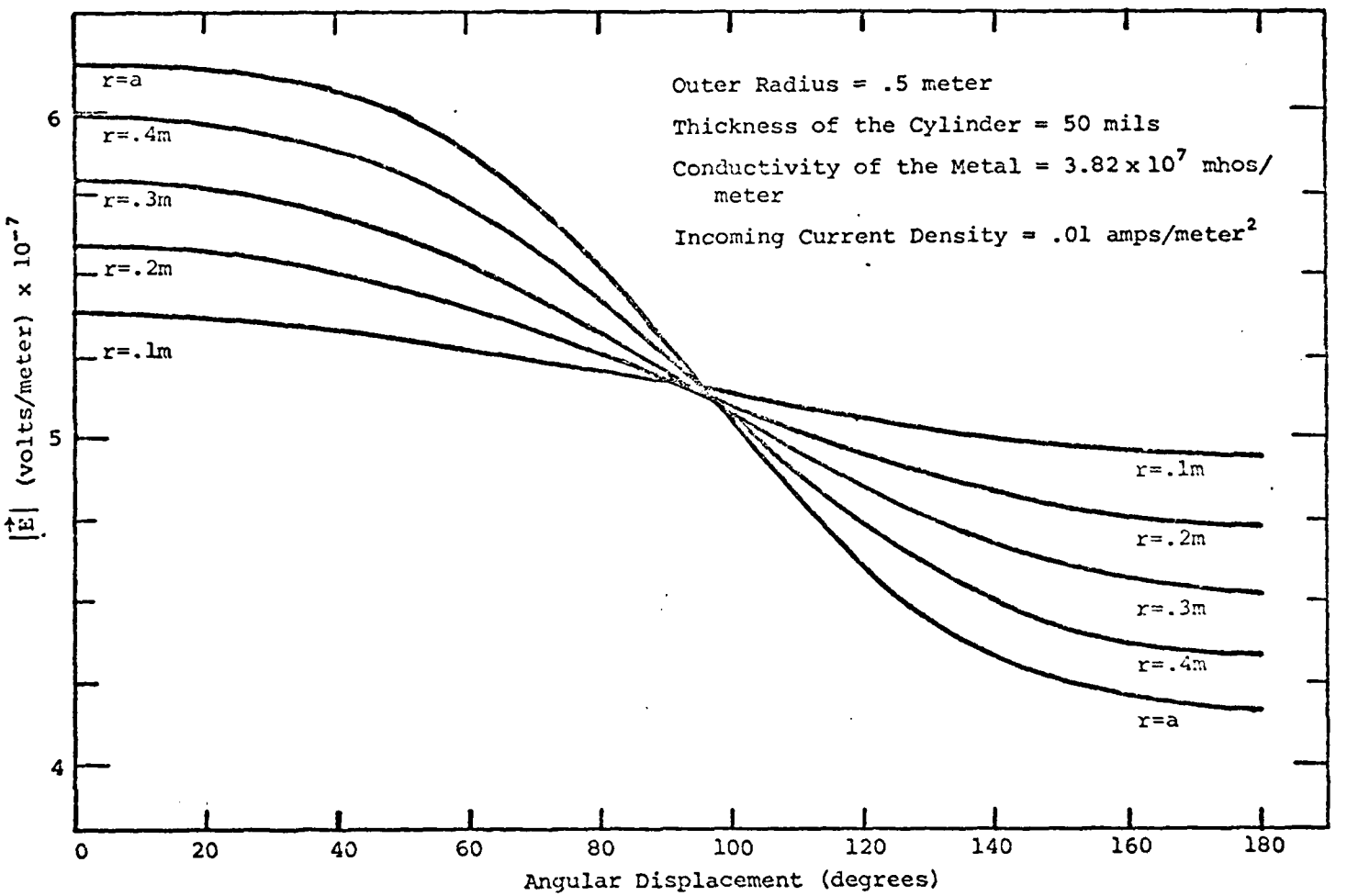


Fig 6-2. Plot of $|\vec{E}|$ vs Angular Displacement for an Aluminum Cylinder 50 mils Thick.

## VII Conclusions and Recommendations

### Conclusions

The results of Chapter IV indicate that it is possible to use the variational method to numerically solve for the potential distribution, provided a fine enough mesh is used.

The results of the Green's function method indicate that it can satisfactorily approximate the potential distribution throughout both regions of the cylinder. Unfortunately, an examination of the electric field predicted by this method was not accomplished. However, since the method was quite successful at predicting the potentials, it seems reasonable to expect similar success in the prediction of the $\vec{E}$-Field.

A comparison of the variational computer program with the Green's function program shows that the variational program requires less execution time, whereas the Green's function program requires less computer storage. Thus, for a problem which cannot be solved analytically, the best numerical approach would depend on whether computer storage or execu- time is more critical to the user.

Lastly, given the representative values for the cylinder's dimensions a d the incoming current density as listed in Chapter VI, the magnitude of the induced $\vec{E}$-Field is on the order of $10^{-7}$ volts/meter.

### Recommendations

1. The computer programs developed in Chapters IV and V only calculate the potential distribution. It would be interesting to develop them one step further to calculate the $\vec{E}$-Field, and then compare the two numerical

methods.

2. To improve the prediction of the electric field inside a spacecraft, the problem should be solved for a finite cylinder with endcaps. One possible model is a thin ellipsoid. This would alleviate the problem of calculating the current flow across the edge of the endcaps.

## Bibliography


1. Churchill, Ruel V. Fourier Series and Boundary Value Problems. New York: McGraw-Hill Book Co., 1963.

2. Courant, Richard, and D. Hilbert. Methods of Mathematical Physics. Vol. I. New York: Interscience Publishers, Inc., 1937.

3. Forray, Marvin J. Variational Calculus in Science and Engineering. New York: McGraw-Hill Book Co., 1968.

4. Gelfand, I.M., and S. V. Fomin. Calculus of Variations. Englewood Cliffs: Prentice-Hall, Inc., 1963.

5. Greenberg, Michael D. Application of Green's Functions in Science and Engineering. Englewood Cliffs: Prentice-Hall, Inc., 1971.

6. Harnwell, G.P. Principles of Electricity and Magnetism. New York: McGraw-Hill Book Co., 1938.

7. Jackson, John D. Classical Electrodynamics. New York: John Wiley and Sons, Inc., 1962.

8. Keller, Charles L. Integral Equation Methods for Two Dimensional Incompressible Flow for Multielement Airfoils. AFFDL-TR-77-27. Wright-Patterson AFB, Ohio: Flight Dynamics Laboratory, April 1977.

9. Lovitt, William V. Linear Integral Equations. New York: Dover Publications, Inc., 1950.

10. Milne, William E. Numerical Calculus. Princeton: Princeton University Press, 1949.

11. Morse, Philip M., and Herman Feshbach. Methods of Theoretical Physics, Part I. New York: McGraw-Hill Book Co., 1953.

12. Smith, Michael G. Introduction to the Theory of Partial Differential Equations. Princeton: D. Van Nostrand Company Inc., 1967.

13. Stakgold, Ivar. Boundary Value Problems of Mathematical Physics, Vol. 1. New York: The Macmillan Co., 1972.

14. Stratton, Julius A. Electromagnetic Theory. New York: McGraw-Hill Book Co., 1941.

15. Weinberger, H. F. Partial Differential Equations. New York: Blaisdell Publishing Co., 1965.

Appendix A

## Derivation of the Solution to $\nabla^2\theta=0$ Using Separation of Variables

The method of separation of variables is used to solve $\nabla^2\phi = 0$. The boundary conditions are then expanded in a Fourier series to obtain an infinite sum expression for $\phi(r,\theta)$.

### Solution in Region I

$$\nabla^2\phi = 0 \tag{A-1}$$

Assume $\phi = R(r)\,\Theta(\theta)$. In cylindrical coordinates

$$\nabla^2\phi = \left[\frac{1}{r}\frac{\partial}{\partial r}\left(r\frac{\partial}{\partial r}\right) + \frac{1}{r^2}\frac{\partial^2}{\partial\theta}\right]R\Theta \tag{A-2}$$

After expanding and multiplying by $r^2$,

$$\frac{r}{R}\frac{d}{dr}\left(r\frac{dR}{dr}\right) = -\frac{1}{\Theta}\frac{d^2\Theta}{d\theta^2} = \lambda^2 \tag{A-3}$$

### Solution if $\lambda^2 = 0$

Solving for R:

$$\frac{d}{dr}\left(r\frac{dR}{dr}\right) = 0 \tag{A-4}$$

$$r\frac{dR}{dr} = A_o \tag{A-5}$$

$$R = A_o \ln r + B_o \tag{A-6}$$

Solving for Θ:

$$\frac{d^2\Theta}{d\theta^2} = 0 \tag{A-7}$$

$$\Theta = C_o\theta + D_o \tag{A-8}$$

Thus

$$\phi = (A_o \ln r + B_o)(C_o\theta + D_o) \tag{A-9}$$

Since $\phi$ is periodic, $C_o$ must be zero. Absorbing $D_o$ in the remaining constants yields

$$\phi = A_o \ln r + B_o \tag{A-10}$$

Solution if $\lambda^2$ is Positive

Solving for R:

$$r\frac{d}{dr}\left(r\frac{dR}{dr}\right) - \lambda^2 R = 0 \tag{A-11}$$

This is Euler's Equation, which can be solved by letting

$$r = e^z \tag{A-12}$$

and

$$\frac{dR}{dr} = \frac{dR}{dz}\frac{dz}{dr} = e^{-z}\frac{dR}{dz} \tag{A-13}$$

The solution is

$$R = Ar^\lambda + Br^{-\lambda} \tag{A-14}$$

Solving for Θ:

$$\frac{d^2\Theta}{d\theta^2} + \lambda\Theta = 0 \tag{A-15}$$

$$\Theta = C\cos\lambda\theta + D\sin\lambda\theta \tag{A-16}$$

For solutions periodic in $2\pi$, $\lambda = n$, where $n = 1,2,3,\ldots$ . Thus the solution for a positive $\lambda^2$ is

$$\phi = \left(A_n r^n + B_n r^{-n}\right)\left(C_n\cos n\theta + D_n\sin n\theta\right) \qquad n = 1,2,\cdots \tag{A-17}$$

The solution when $\lambda^2$ is negative can be ignored because it contains sinh $\theta$ and cosh $\theta$ terms, which are not periodic.

Thus, the general solution is,

$$\phi = A_o \ln r + B_o +$$

$$\sum_{n=1}^{\infty}\left[\left(A_n r^n + B_n r^{-n}\right)\cos n\theta + \left(C_n r^n + D_n r^{-n}\right)\sin n\theta\right] \tag{A-18}$$

The boundary conditions are

$$\frac{\partial\phi}{\partial r}(a,\theta) = 0$$

$$\frac{\partial\phi}{\partial r}(b,\theta) = f(\theta) = \begin{cases} \frac{I}{\sigma}\left(\cos\theta - \frac{1}{\pi}\right) & -\frac{\pi}{2} \le \theta \le \frac{\pi}{2} \\ -\frac{I}{\sigma\pi} & \frac{\pi}{2} \le \theta \le \frac{3\pi}{2} \end{cases}$$

Applying the first boundary condition yields

$$A_o = 0 \tag{A-19a}$$

$$A_n a^{n-1} - B_n a^{-n-1} = 0 \tag{A-19b}$$

$$C_n a^{n-1} - D_n a^{-n-1} = 0 \tag{A-19c}$$

Applying the second boundary condition yields

$$\sum_{n=1}^{\infty}\left[\left(nA_n b^{n-1} - nB_n b^{-n-1}\right)\cos n\theta + \left(nC_n b^{n-1} - nD_n b^{-n-1}\right)\sin n\theta\right] = f(\theta) \qquad \text{(A-20)}$$

The Fourier expansion for f(θ) is given in Eqn (B-9), Appendix B. Since there are no sine terms in the expansion

$$nC_n b^{n-1} - nD_n b^{-n-1} = 0 \qquad \text{(A-21)}$$

Solving this equation simultaneously with Eqn (A-19c) yields

$$C_n = D_n = 0 \qquad \text{(A-22)}$$

Equating coefficients of the cosine terms in Eqns (A-20) and (B-9) for n = 1 yields

$$A_1 - B_1 b^{-2} = \frac{I}{2\sigma} \qquad \text{(A-23)}$$

Solving this equation simultaneously with Eqn (A-19b) for n = 1 yields

$$A_1 = \frac{I b^2}{2\sigma(b^2 - a^2)} \qquad \text{(A-24a)}$$

$$B_1 = \frac{I a^2 b^2}{2\sigma(b^2 - a^2)} \qquad \text{(A-24b)}$$

Equating coefficients of the cosine terms in Eqns (A-20) and (B-9) for n = 2,4,6,... yields

$$nA_n b^{n-1} - nB_n b^{-n-1} = \frac{(-1)^{\frac{n-2}{2}}\, 2I}{\sigma\pi(n^2-1)} \qquad n = 2, 4, 6, \ldots \qquad \text{(A-25)}$$

Solving this equation simultaneously with Eqn (A-19b) for n>1 yields

$$A_n = \frac{(-1)^{\frac{n-2}{2}} 2I b^{n+1}}{n\sigma\pi(n^2-1)(b^{2n}-a^{2n})} \qquad n = 2,4,6,\cdots \qquad \text{(A-26a)}$$

$$B_n = \frac{(-1)^{\frac{n-2}{2}} 2I a^{2n} b^{n+1}}{n\sigma\pi(n^2-1)(b^{2n}-a^{2n})} \qquad n = 2,4,6,\cdots \qquad \text{(A-26b)}$$

The coefficients of $\cos(n\theta)$ are zero for $n = 3,5,7,\ldots$ . Thus $A_n = B_n = 0$ when $n = 3,5,7,\ldots$ .

The equation for $\phi(r,\theta)$ can now be found by substituting Eqns (A-19a), (A-24), and (A-26) into Eqn (A-18):

$$\phi(r,\theta) = \frac{I b^2 \cos\theta}{2\sigma(b^2-a^2)}\left(r + \frac{a^2}{r}\right) + \frac{(-1)^{\frac{n-2}{2}} 2I b^{n+1} \cos n\theta}{n\sigma\pi(n^2-1)(b^{2n}-a^{2n})}\left(r^n + \frac{a^{2n}}{r^n}\right) \qquad n = 2,4,6,\cdots \qquad \text{(A-27)}$$

Equation (2-27) can be rewritten with an infinite sum by substituting 2n for n.

$$\phi_I(r,\theta) = \frac{I b^2 \cos\theta}{2\sigma(b^2-a^2)}\left(r + \frac{a^2}{r}\right) + \sum_{n=1}^{\infty} \frac{(-1)^{n-1} I b^{2n+1} \cos(2n\theta)}{n\sigma\pi(4n^2-1)(b^{4n}-a^{4n})}\left(r^{2n} + \frac{a^{4n}}{r^{2n}}\right) \qquad \text{(A-28)}$$

Equation (A-28) gives the potentials throughout Region I. The constant $B_o$ in Eqn (A-18) has been set to zero. Since $\nabla\phi$ is the term of interest, any constant term would vanish when the gradient is calculated.

Solution in Region II

The equation to be solved is

$$\nabla^2\phi = 0 \tag{A-29}$$

with boundary condition $\phi\ (a,\theta) = f(a,\theta)$ where $f(a,\theta)$ is given by the solution to Region I.

Using the same procedure as before, the general solution is

$$\phi = A_o \ln r + B_o + \sum_{n=1}^{\infty}\left[\left(A_n r^n + B_n r^{-n}\right)\cos n\theta + \left(C_n r^n + D_n r^{-n}\right)\sin n\theta\right] \tag{A-30}$$

Since $\phi$ must be bounded at $r = 0$, $A_o = B_n = D_n = 0$. Also, the additive constant, $B_o$, is set to 0. Since the gradient of $\phi$ is desired, $B_o$ would drop out anyway. Thus, the general solution is reduced to

$$\phi = \sum_{n=1}^{\infty} A_n r^n \cos n\theta + C_n r^n \sin n\theta \tag{A-31}$$

Applying the boundary condition at $r = a$ yields

$$\sum_{n=1}^{\infty}\left[A_n a^n \cos(n\theta) + C_n a^n \sin(n\theta)\right] =$$

$$\frac{2\,[illegible]\cos\theta}{2\sigma\pi(b^2 - a^2)} + \sum_{n=1}^{\infty}\frac{(-1)^{n-1} I b^{2n+1}\cos(2n\theta)(2a^{2n})}{n\sigma\pi(4n^2-1)(b^{4n} - a^{4n})} \tag{A-32}$$

Since there are no sine terms in the right-hand side, $C_n = 0$.

Equating the coefficients of cos $\theta$ for $n = 1$,

$$A_1 a = \frac{I b^2 a}{\sigma(b^2 - a^2)} \tag{A-33}$$

which simplifies to

$$A_1 = \frac{I b^2}{\sigma(b^2 - a^2)} \tag{A-34}$$

Equating the coefficients of cos $\theta$ for $n = 2,4,6,\ldots,$

$$\sum_{n=1}^{\infty} A_{2n} a^{2n} = \sum_{n=1}^{\infty} \frac{(-1)^{n-1} 2I b^{2n+1} a^{2n}}{n\sigma\pi(4n^2-1)(b^{4n}-a^{4n})} \tag{A-35}$$

Solving for the constant A,

$$A_{2n} = \frac{(-1)^{n-1} 2I b^{2n+1}}{n\sigma\pi(4n^2-1)(b^{4n}-a^{4n})} \tag{A-36}$$

When n = 3,5,7,... the constant coefficients are zero.

Substituting Eqns (A-34) and (A-36) into Eqn (A-31) yields the potential distribution for Region II,

$$\Phi_{II}(r,\theta) = \frac{I b^2 r \cos\theta}{\sigma(b^2-a^2)} + \sum_{n=1}^{\infty} \frac{(-1)^{n-1} 2I b^{2n+1} r^{2n} \cos(2n\theta)}{n\sigma\pi(4n^2-1)(b^{4n}-a^{4n})} \tag{A-37}$$

Appendix B

## Fourier Expansion of the Boundary Conditions

In Appendix A a solution for $\nabla^2\phi = 0$ was derived in terms of an infinite sum of sine and cosine terms. The boundary conditions, represented as $f(\theta)$, were then expanded in a Fourier series to determine the coefficients for the sine and cosine terms in the solution. The purpose of this appendix is to present the Fourier analysis used to determine those coefficients.

The solution at r = b can be written in the form, (Ref: Eqn (A-20)),

$$\sum_{n=1}^{\infty} \left[E_n \cos(n\theta) + F_n \sin(n\theta)\right] = f(\theta) \qquad \text{(B-1)}$$

where

$$f(\theta) = \begin{cases} \frac{I}{\sigma}\left(\cos\theta - \frac{1}{\pi}\right) & -\frac{\pi}{2} \le \theta \le \frac{\pi}{2} \\ \frac{-I}{\sigma\pi} & \frac{\pi}{2} \le \theta \le \frac{3\pi}{2} \end{cases}$$

Since $f(\theta)$ contains only even functions, its Fourier expansion will not have any sine terms. Hence $F_n = 0$ in Eqn (B-1).

The expression for $E_n$ is

$$E_n = \frac{1}{L}\int f(\theta)\cos\left(\frac{n\pi\theta}{L}\right)d\theta \quad n = 1, 2, 3, \cdots \qquad \text{(B-2)}$$

where 2L = Period. For this problem the period is $2\pi$.

When the equations for $f(\theta)$ are substituted in Eqn (B-2) and integrated over the appropriate limits, the following equation results,

$$E_n = \frac{1}{\pi}\int_{-\frac{\pi}{2}}^{\frac{\pi}{2}} \frac{I}{\sigma}\left(\cos\theta - \frac{1}{\pi}\right)\cos(n\theta)\,d\theta \quad +$$

$$\frac{1}{\pi}\int_{\frac{\pi}{2}}^{\frac{3\pi}{2}} \frac{-I}{\sigma\pi}\cos(n\theta)\,d\theta \qquad n=0,1,2,\cdots \tag{B-3}$$

When n = 0 the above expression is zero. Hence there is no constant term in the Fourier expansion. Eqn (B-3) can be rewritten as

$$E_n = \frac{I}{\sigma\pi}\int_{-\frac{\pi}{2}}^{\frac{\pi}{2}}\left[\cos\theta\cos(n\theta) - \frac{\cos(n\theta)}{\pi}\right]d\theta \quad -$$

$$\frac{I}{\sigma\pi^2}\int_{\frac{\pi}{2}}^{\frac{3\pi}{2}} \cos(n\theta)\,d\theta \qquad n=1,2,3,\cdots \tag{B-4}$$

Integration of this equation yields

$$E_n = \begin{cases} \dfrac{I}{\sigma\pi}\left[\dfrac{\theta}{2} + \dfrac{\sin(2\theta)}{4} - \dfrac{\sin\theta}{\pi}\right]_{-\frac{\pi}{2}}^{\frac{\pi}{2}} - \dfrac{I}{\sigma\pi^2}\left[\sin\theta\right]_{\frac{\pi}{2}}^{\frac{3\pi}{2}} & n=1 \\ \dfrac{I}{\sigma\pi}\left[\dfrac{\sin(n-1)\theta}{2(n-1)} + \dfrac{\sin(n+1)\theta}{2(n+1)} - \dfrac{\sin(n\theta}{n\pi}\right]_{-\frac{\pi}{2}}^{\frac{\pi}{2}} - \dfrac{I}{\sigma\pi^2}\left[\dfrac{\sin(n\theta)}{n}\right]_{\frac{\pi}{2}}^{\frac{3\pi}{2}} & n>1 \end{cases} \tag{B-5}$$

$$E_n = \begin{cases} \frac{I}{\sigma\pi}\left[\frac{\pi}{2} - \frac{2}{\pi}\right] - \frac{I}{\sigma\pi^2}\left[-2\right] & n = 1 \\ \frac{I}{\sigma\pi}\left[\frac{1}{n-1} - \frac{1}{n+1}\right] & n = 2, 6, 10, \cdots \\ \frac{I}{\sigma\pi}\left[\frac{-1}{n-1} + \frac{1}{n+1}\right] & n = 4, 8, 12, \cdots \\ \frac{I}{\sigma\pi}\left[\frac{2}{n\pi}\right] - \frac{I}{\sigma\pi^2}\left[\frac{2}{n}\right] & n = 3, 7, 11, \cdots \\ \frac{I}{\sigma\pi}\left[\frac{-2}{n\pi}\right] - \frac{I}{\sigma\pi^2}\left[\frac{-2}{n}\right] & n = 5, 9, 13, \cdots \end{cases} \quad \text{(B-6)}$$

$$E_n = \begin{cases} \frac{I}{2\pi} & n = 1 \\ \frac{2I}{\sigma\pi(n^2-1)} & n = 2, 6, 10, \cdots \\ \frac{-2I}{\sigma\pi(n^2-1)} & n = 4, 8, 12, \cdots \\ 0 & n = 3, 5, 7, \cdots \end{cases} \quad \text{(B-7)}$$

$$E_n = \begin{cases} \frac{I}{2\pi} & n = 1 \\ \frac{(-1)^{\frac{n-2}{2}}\, 2I}{\sigma\pi(n^2-1)} & n = 2, 4, 6, \cdots \\ 0 & n = 3, 5, 7, \cdots \end{cases} \quad \text{(B-8)}$$

When Eqns (B-1) and B-8) are combined and simplified, the Fourier expansion for $f(\theta)$ over the interval 0 to $2\pi$ can be written

$$f(\theta) = \frac{I\cos\theta}{2\sigma} + \frac{(-1)^{\frac{n-2}{2}}\, 2I\cos(n\theta)}{\sigma\pi\,(n^2-1)} \qquad n = 2, 4, 6, \cdots \qquad \text{(B-9)}$$

This expansion was used with Eqn (A-18) to evaluate the constants in the general solution for $\phi(r,\theta)$.

Appendix C

## Computer Program to Calculate the Magnitude of the $\vec{E}$-Field

This program computes the magnitude of the electric field at various points throughout the hollow portion of the cylinder. It is essentially a program of Eqn (3-5).

Cards 1 - 28: Self explanatory.

Card 29: The value of the inner radius is calculated.

Cards 33, 34: These cards convert the angular and radial increments into DO LOOP indices.

Card 35: A DO LOOP is initialized which spans all the angular increments.

Card 36: THETA is the angular displacement of each radial line.

Card 37: A DO LOOP is initialized which spans all the points along a given radial line.

Card 38: R is the radial displacement of the point being calculated.

Card 39: This card ensures that all points lie in the hollow portion of the cylinder.

Card 40: THETA is converted into radians.

Cards 41 - 49: The radial component of the electric field is calculated as given in Eqn (3-5). The summation is continued until two successive values differ by less than .0001.

Cards 50 - 58: The angular component of the electric field is calculated as given in Eqn (3-5). The summation is continued until two successive values differ by less than .0001.

Card 59: The magnitude of the $\vec{E}$-Field is calculated.

Card 60: THETA is converted back to degrees.

```
      PROGRAM EFIELD(INPUT,OUTPUT)
C     R=OUTER RADIUS OF THE CYLINDRICAL SHELL IN METERS
C     THICK=THICKNESS OF THE CYLINDRICAL SHELL IN MILS.
C     SIGMA=CONDUCTIVITY OF THE METALLIC SHELL IN
C     MHOS/METER.
C     CI=INCOMING CURRENT DENSITY IN AMPS/METER**2
C     DA=ANGULAR INCREMENT IN DEGREES
C     DR=RADIAL INCREMENT IN METERS
C     R=RADIAL COORDINATE, IN METERS, OF A POINT IN THE
C     HOLLOW PORTION OF THE CYLINDER WHERE THE STRENGTH
C     OF THE E-FIELD IS TO BE CALCULATED.
C     THETA=ANGULAR COORDINATE IN DEGREES FOR THAT SAME
C     POINT.
C     E=MAGNITUDE OF THE E-FIELD IN VOLTS/METER
   90 FORMAT(1X,F7.3,5X,F4.0,7X,E11.4)
   91 FORMAT(1X,"OUTER RADIUS=",F5.2," METERS")
   92 FORMAT(1X,"THICKNESS OF THE CYLINDRICAL SHELL=",
     1F5.1," MILS")
   93 FORMAT(1X,"CONDUCTIVITY OF THE METAL=",E11.4,
     1" MHOS/METER")
   94 FORMAT(1X,"INCOMING CURRENT DENSITY=",E11.4,
     1" AMPS/METER**2")
      PI=3.14159265359
   10 READ*,R,THICK,SIGMA,CI,DA,DR
      IF(EOF(5LINPUT).NE.1)STOP
      PRINT*," "
      WRITE 91,R
      WRITE 92,THICK
      A=R-THICK*25.4E-03
      WRITE 93,SIGMA
      WRITE 94,CI
      PRINT*," R (M)    THETA (DEG)    E-FIELD (V/M)"
```

```
      KA=180/DA+1
      KR=A/DR+2
      DO 5 I=1,KA
      THETA=(I-1)*DA
      DO 5 J=1,KR
      R=(J-1)*DR
      IF(R.GT.A)R=A
      THETA=THETA*2.*PI/360.
      RAD=0.
      DO 1 N=1,50
      SAVE=RAD
      RAD=RAD+(-1.)**(N-1)*4.*CI*B**(2*N+1)*R**(2*N-1)*
     1      COS(2*N*THETA)/
     2      (SIGMA*PI*(2.*N*N-1.)*(B**(4*N)-A**(4*N)))
      IF(ABS(SAVE-RAD)._T..0001.AND.N.GT.1)GO TO 2
1     CONTINUE
2     RAD=-RAD-CI*B*B*COS(THETA)/(SIGMA*(B*B-A*A))
      ANG=0.
      DO 3 N=1,50
      SAVE=ANG
      ANG=ANG+(-1.)**(N-1)*4.*CI*B**(2*N+1)*R**(2*N-1)*
     1      SIN(2*N*THETA)/
     2      (SIGMA*PI*(2.*N*N-1.)*(B**(4*N)-A**(4*N)))
      IF(ABS(SAVE-ANG)._T..0001.AND.N.GT.1)GO TO 4
3     CONTINUE
4     ANG=ANG+CI*B*B*SIN(THETA)/(SIGMA*(B*B-A*A))
      E=SQRT(RAD*RAD+ANG*ANG)
      THETA=THETA*360./2./PI
5     WRITE 99,R,THETA,E
      GO TO 10
      END
```

Appendix D

## Derivation of the Minimization Functional

This appendix contains the derivation of the functional, Eqn (4-1), which was minimized in the variational approach. The discussion method used will be to first present a general functional for the problem being solved. This will be followed by a presentation of a specific functional compatible with the given boundary conditions as listed in Chapter II. It will then be shown that this functional, $J[\phi]$, is a minimum by adding another non-zero function, v, to $\phi$, and showing that $J[\phi+v] > J[\phi]$.

The general problem is listed in Eqn (D-1). The equation is inhomogeneous and must satisfy mixed boundary conditions.

$$\nabla^2\phi = S \tag{D-1}$$

On the Inner Surface,

$$\left.\frac{\partial\phi}{\partial r}\right|_{r=a} + \sigma_1\phi = g_1$$

On the Outer Surface,

$$\left.\frac{\partial\phi}{\partial r}\right|_{r=b} + \sigma_2\phi = g_2$$

The applicable functional is

$$J[\phi] = \frac{1}{2}\int_A [(\nabla\phi)^2 - 2\phi S]\,dA + \frac{1}{2}\int_{S_{inner}} (\sigma_1\phi^2 - 2\phi g_1)\,ds + \frac{1}{2}\int_{S_{outer}} (\sigma_2\phi^2 - 2\phi g_2)\,ds \tag{D-2}$$

For the problem as derived in Chapter II, $S = \sigma_1 = \sigma_2 = g_1 = 0$, and $g_2 = f(\theta)$. So Eqn. (D-2) becomes

$$J[\phi] = \frac{1}{2}\int_A (\nabla\phi)^2 dA + \frac{1}{2}\int_\theta -2\phi f(\theta) b\, d\theta \qquad \text{(D-3)}$$

where the second integral has been converted to an integral over $\theta$ by use of the relation $ds = rd\theta = bd\theta$.

It will now be shown that if a non-zero function, v, is added to $\phi$, then $J[\phi+v] > J[\phi]$. (Both $\phi$ and v belong to the class of functions which has a continuous second derivative.) If this is true, then Eqn. (D-3) is the correct functional to be minimized.

$$J[\phi+v] = \frac{1}{2}\int_A [(\nabla\phi)^2 + 2\nabla\phi\cdot\nabla v + (\nabla v)^2] dA +$$

$$\frac{1}{2}\int_\theta -2(\phi+v) f(\theta) b\, d\theta \qquad \text{(D-4)}$$

$$= J[\phi] + \frac{1}{2}\int_A (\nabla v)^2 dA + \int_A \nabla\phi\cdot\nabla v\, dA -$$

$$\int_\theta v f(\theta) b\, d\theta \qquad \text{(D-5)}$$

The second term is positive for any non-zero v. Thus, if it can be shown that terms three and four are zero for any v, then $J[\phi+v]$ is greater than $J[\phi]$.

An identity from vector analysis gives the relation

$$\nabla\cdot(w\vec{A}) = w\nabla\cdot\vec{A} + \vec{A}\cdot\nabla\vec{w} \tag{D-6}$$

By letting $v = w$ and $\nabla\phi = \vec{A}$, the above equation becomes

$$\nabla\cdot(V\nabla\phi) = V\nabla\cdot\nabla\phi + \nabla\phi\cdot\nabla V \tag{D-7}$$

Thus

$$\nabla\phi\cdot\nabla V = \nabla\cdot(V\nabla\phi) - V\nabla\cdot\nabla\phi \tag{D-8}$$

Integrating Eqn (D-8) over the area of interest yields

$$\int_A(\nabla\phi\cdot\nabla V)\,dA = \int_A\nabla\cdot(V\nabla\phi)\,dA - \int_A(V\nabla\cdot\nabla\phi)\,dA \tag{D-9}$$

Through application of the divergence theorem, the first integral on the right side can be expressed as

$$\int_A\nabla\cdot(V\nabla\phi)\,dA = \int_{S_{inner}} V\frac{\partial\phi}{\partial n}\,ds + \int_{S_{outer}} V\frac{\partial\phi}{\partial n}\,ds \tag{D-10}$$

Substituting back into Eqn (D-9) yields

$$\int_A(\nabla\phi\cdot\nabla V)\,dA = \int_{S_{outer}} V\frac{\partial\phi}{\partial n}\,ds + \int_A(V\nabla\cdot\nabla\phi)\,dA \tag{D-11}$$

Note: $\frac{\partial\phi}{\partial n} = \frac{\partial\phi}{\partial r} = 0$ on the inner boundary.

As stated in the discussion after Eqn (D-5), it must be shown that

$$\int_A(\nabla\phi\cdot\nabla V)\,dA - \int_\theta Vf(\theta)\,b\,d\theta = 0 \tag{D-12}$$

Substituting Eqn (D-11) into first integral yields

$$\int_{\theta} v \frac{\partial \phi}{\partial r} b\, d\theta - \int_{A} v \nabla \cdot \nabla \phi \, dA - \int_{\theta} v f(\theta) b\, d\theta \stackrel{?}{=} 0 \qquad \text{(D-13)}$$

where the integral over S has been converted to an integral over $\theta$ using $ds = rd\theta = bd\theta$.

Equation (D-13) can be rewritten as

$$\int_{A} v \nabla^2 \phi \, dA + \int_{\theta} v \left[ \frac{\partial \phi}{\partial r} - f(\theta) \right] b\, d\theta \stackrel{?}{=} 0 \qquad \text{(D-14)}$$

The first integral is zero from the initial equation $\nabla^2 \phi = 0$. The second term is zero from the outer boundary condition. Thus $J[\phi+v] \; J[\phi]$ for any non-zero v. Hence Eqn (D-3) is the proper minimization functional for the given equation with Neumann boundary conditions.

## Appendix E

### Reduction of the Coefficient Matrix

This appendix contains an explanation of the use of symmetry in reducing the size of the variational matrix problem. Also included, is a discussion of an attempt to further reduce the matrix through "decoupling".

#### Use of Symmetry

The coefficient matrix, $\underline{A}$, generated by Eqns (4-9), (4-10), and (4-11) becomes very large as the mesh becomes finer and finer. However, it is possible to reduce the size of this matrix by taking advantage of the symmetry of the problem.

Figure E-1 illustrates a 5 x 8 mesh over the shell portion of the cylinder. A mesh this size was chosen for explanation because it illustrates the salient features of the matrix reduction without becoming too cumbersome. The points of discussion can be generalized to any size matrix which has an odd number of radial mesh points, NR, and an even number of angular mesh points, NA. The matrix generated by Eqns (4-9), (4-10), and (4-11) has the form

$$\begin{bmatrix} d & f & g & o & o & o & g & f \\ f & e & f & h & o & o & o & h \\ g & f & d & f & g & o & o & o \\ o & h & f & e & f & h & o & o \\ o & o & g & f & d & f & g & o \\ o & o & o & h & f & e & f & h \\ g & o & o & o & g & f & d & f \\ f & h & o & o & o & h & f & e \end{bmatrix} \qquad \text{(E-1)}$$

The terms d, e, f, g, and h are block submatrices of size NR x NR.

Since the incoming current density is the same above and below the line $\theta = 0$, the values of the potential will be the same for those mesh points

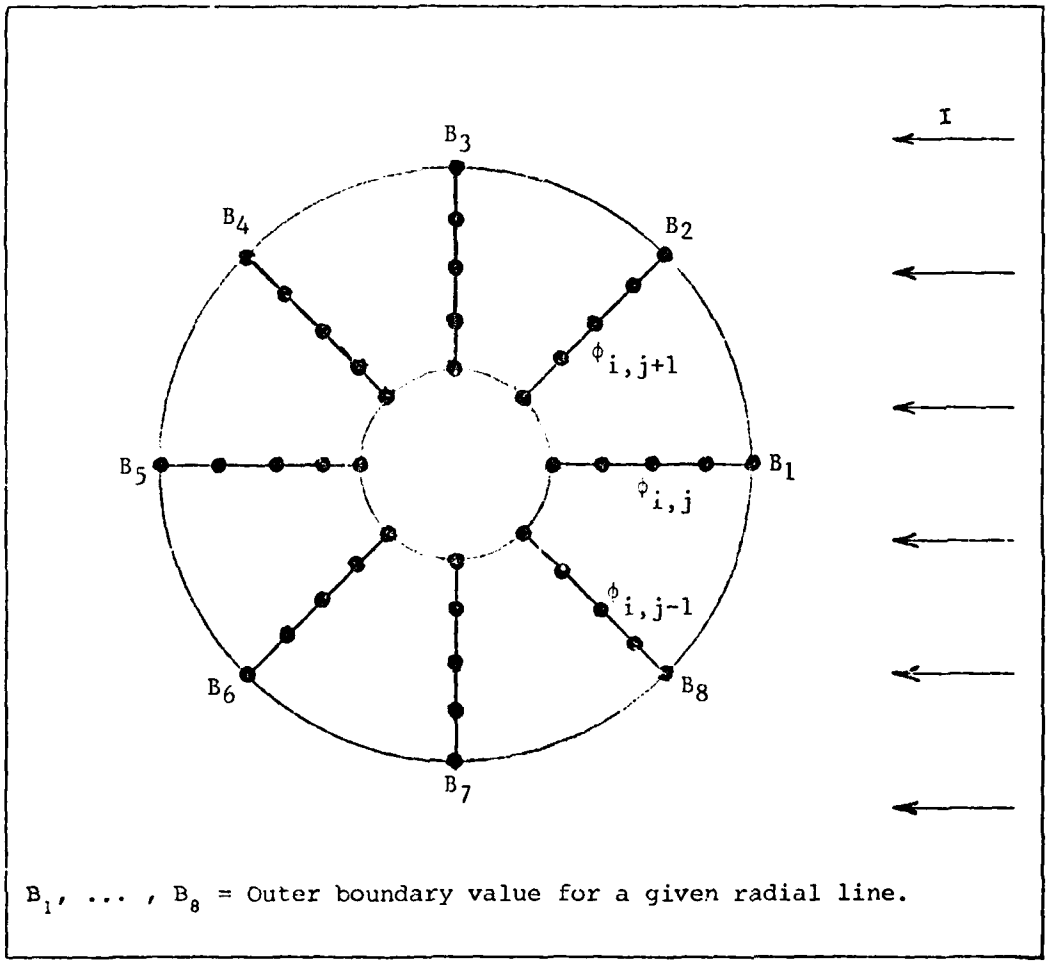


$B_1$, ... , $B_8$ = Outer boundary value for a given radial line.

Fig E-1. Sample Mesh for Calculating $\phi$ in the Cylindrical Shell.

which are symmetric about the line $\theta = 0$, (i.e., $\phi_{i,j+1} = \phi_{i,j-1}$). Thus, the number of mesh points actually calculated can be cut approximately in half.

The matrix form of the problem is

$$\underline{\underline{A}}\,\underline{\phi} = \underline{B} \tag{E-2}$$

A new variable $\Psi$, is defined as

$$\underline{\Psi} = \underline{\underline{O}}^{-1}\underline{\phi} \tag{E-3}$$

where

$$\Psi_{i,K} = \frac{1}{2}\left(\phi_{i,j} + \phi_{i,-j}\right) \qquad K = j = 0,1,2,\cdots,\frac{NA}{2}$$

$$\Psi_{i,K} = \phi_{i,j} - \phi_{i,-j} \qquad j = K - \frac{NA}{2} = 1,2,\cdots \frac{NA}{2} - 1$$

Thus $\underline{\phi} = \underline{\underline{O}}\,\underline{\Psi}$, and Eqn (E-2) becomes

$$\underline{\underline{A}}\,\underline{\underline{O}}\,\underline{\Psi} = \underline{B} \tag{E-4}$$

Pre-multiplying Eqn (E-4) by $\underline{\underline{\tilde{O}}}$ yields a new matrix problem

$$\underline{\underline{\tilde{O}}}\,\underline{\underline{A}}\,\underline{\underline{O}}\,\underline{\Psi} = \underline{\underline{\tilde{O}}}\,\underline{B} \tag{E-5}$$

The form of $\underline{\underline{O}}$ is such that

$$\underline{\underline{O}}^{-1}\underline{B} = \begin{bmatrix} b' \\ 0 \end{bmatrix} \tag{E-6}$$

That is, all the terms of $\underline{B}$ lying below the axis of symmetry become zero. As can be seen from Fig E-1, the values of $\underline{B}$ which are equal are $B_2 = B_8$, $B_3 = B_7$, and $B_4 = B_6$. Since $B_6$, $B_7$, and $B_8$ all lie below the axis of symmetry, they must be set to zero. Thus, it is necessary to find an $\underline{\underline{O}}^{-1}$ matrix which, when operating on $\underline{B}$, sets $B_6 = B_7 = B_8 = 0$.

An $\underline{O}^{-1}$ matrix which satisfies this condition is

$$\begin{bmatrix} 1 & 0 & 0 & 0 & 0 & 0 & 0 & 0 \\ 0 & \frac{1}{2} & 0 & 0 & 0 & 0 & 0 & \frac{1}{2} \\ 0 & 0 & \frac{1}{2} & 0 & 0 & 0 & \frac{1}{2} & 0 \\ 0 & 0 & 0 & \frac{1}{2} & 0 & \frac{1}{2} & 0 & 0 \\ 0 & 0 & 0 & 0 & 1 & 0 & 0 & 0 \\ 0 & 0 & 0 & 1 & 0 & -1 & 0 & 0 \\ 0 & 0 & 1 & 0 & 0 & 0 & -1 & 0 \\ 0 & 1 & 0 & 0 & 0 & 0 & 0 & -1 \end{bmatrix} \begin{bmatrix} B_1 \\ B_2 \\ B_3 \\ B_4 \\ B_5 \\ B_6 \\ B_7 \\ B_8 \end{bmatrix} = \begin{bmatrix} B_1 \\ B_2 \\ B_3 \\ B_4 \\ B_5 \\ 0 \\ 0 \\ 0 \end{bmatrix} \qquad \text{(E-7)}$$

Of course the $\underline{O}^{-1}$ matrix can be expanded to accommodate any $\underline{B}$ vector generated by an even number of angular mesh points.

The effect of the operations $\tilde{\underline{O}}\,\underline{A}\,\underline{O}$ and $\underline{O}\underline{B}$ can be calculated once $O^{-1}$ is known. The matrix generated is significantly smaller than the original coefficient matrix.

$$\tilde{\underline{O}}\,\underline{A}\,\underline{O} = \begin{bmatrix} d & 2f & 2g & 0 & 0 & 0 & 0 & 0 \\ 2f & 2k & 2f & 2h & 0 & 0 & 0 & 0 \\ 2g & 2f & 2d & 2f & 2g & 0 & 0 & 0 \\ 0 & 2h & 2f & 2k & 2f & 0 & 0 & 0 \\ 0 & 0 & 2g & 2f & d & 0 & 0 & 0 \\ 0 & 0 & 0 & 0 & 0 & x & x & x \\ 0 & 0 & 0 & 0 & 0 & x & x & x \\ 0 & 0 & 0 & 0 & 0 & x & x & x \end{bmatrix} \qquad \text{(E-8)}$$

where $k = e+h$.

The lower right submatrices, indicated with an x, are unimportant because the corresponding terms in $\underline{B}$ will be zero through the operation $\tilde{\underline{O}}\,B$.

$$\tilde{\underline{O}}\,\underline{B} = \begin{bmatrix} B_1 \\ 2B_2 \\ 2B_3 \\ 2B_4 \\ B_5 \\ 0 \\ 0 \\ 0 \end{bmatrix} \qquad \text{(E-9)}$$

Thus, the matrix problem reduces to

$$\begin{bmatrix} d & 2f & 2g & 0 & 0 \\ 2f & 2k & 2f & 2h & 0 \\ 2g & 2f & 2d & 2f & 2g \\ 0 & 2h & 2f & 2k & 2f \\ 0 & 0 & 2g & 2f & d \end{bmatrix} \underline{\Psi} = \begin{bmatrix} B_1 \\ 2B_2 \\ 2B_3 \\ 2B_4 \\ B_5 \end{bmatrix} \qquad \text{(E-10)}$$

The matrix on the left side is decomposed via a Choleski decomposition, and the resulting equation is solved using the procedure outlined in Eqns (4-6) and (4-7). Also, with the definition of $\Psi$ as indicated in Eqn (E-3), the values of $\Psi$ calculated from Eqn (E-10) are actually the values of the potential, $\phi$.

Decoupling

An attempt was made to reduce the large matrix problem to two smaller problems by "decoupling". If Eqn (4-11b) is used to approximate the angular derivatives at each mesh point, every other radial line is linked together. All the mesh points along the even-numbered radials are linked together, and all the mesh points along the odd-numbered radials are linked together. Thus, for the sample mesh in Fig E-1, the 40 x 40 matrix could be reduced to two 20 x 20 matrices. (These could be further reduced through the use of symmetry.)

This technique did not work because, as explained in Chapter IV, use of Eqn (4-11b) is an improper way of approximating the angular derivatives. Both left and right derivatives must be approximated at each mesh point, and this destroys the "decoupling" nature of the matrix.

Appendix F

## Importance of Natural Boundary Conditions when Minimizing a Functional

The first attempt at the variational approach was to minimize the functional

$$S = \frac{1}{2}\int_A (\nabla\Phi)^2 dA \qquad \text{(F-1)}$$

and impose the Neumann boundary conditions through the use of a Lagrange Multiplier, $\lambda$.

In matrix form, the attempt was to minimize

$$S = \frac{1}{2}\,\underline{\tilde{\Phi}}\,\underline{\underline{A}}\,\underline{\Phi} \qquad \text{(F-2)}$$

subject to the constraint

$$\underline{\underline{B}}\,\underline{\Phi} - \underline{a} = 0 \qquad \text{(F-3)}$$

where $\underline{\underline{B}}$ and $\underline{a}$ were determined from the quadrature formulae and the boundary conditions.

Imposing Eqn (F-3) on Eqn (F-2) through the use of Lagrange Multipliers led to a new functional, S*:

$$S^* = \frac{1}{2}\,\underline{\tilde{\Phi}}\,\underline{\underline{A}}\,\underline{\Phi} + \underline{\tilde{\lambda}}\,(\underline{\underline{B}}\,\underline{\Phi} - \underline{a}) \qquad \text{(F-4)}$$

(Note: $\tilde{\lambda}$ is used to be consistent with the definition of matrix multiplication.)

Then S* was varied with respect to $\tilde{\phi}$ and $\tilde{\lambda}$.

$$\frac{\delta S^*}{\delta \tilde{\Phi}} = \underline{\underline{A}}\,\underline{\Phi} + \underline{\underline{\tilde{B}}}\,\underline{\lambda} = 0 \qquad \text{(F-5)}$$

$$\frac{\delta S^*}{\delta \tilde{\lambda}} = \underline{\underline{B}}\,\underline{\Phi} - \underline{a} = 0 \qquad \text{(F-6)}$$

Matrix Eqns (F-5) and (F-6) were then solved to determine $\phi$. Figure F-1 illustrates the results of the calculation.

The error in the above procedure is that the functional in Eqn (F-1) has inherent in it homogeneous Neumann boundary conditions. This can be seen by setting $g_2$ equal to zero in Eqn (D-3). Thus the functional was trying to minimize an equation with inherent (natural) homogeneous Neumann boundary conditions on both boundaries. But, through the use of Lagrange Multipliers, it was also being told to satisfy inhomogeneous Neumann conditions on the outer boundary. These two conflicting conditions produced the unsatisfactory curve in Fig F-1.

An investigation was also made to determine the effect of imposing Neumann boundary with Lagrange Multipliers on a functional in which the Neumann conditions were already imposed through the natural boundary conditions. The following one dimensional problem was used for this purpose:

$$\frac{1}{r}\frac{d}{dr}\left(r\frac{dR}{dr}\right) - \frac{R}{r^2} = 0 \qquad \text{(F-7)}$$

$$R'(a) = 0$$

$$R'(b) = 1$$

The corresponding functional is

$$J[R] = \frac{1}{2}\int_r \left[(R')^2 + \frac{R^2}{r^2}\right] r\,dr \; +$$

$$\frac{1}{2}\left[-2R(b)(1)\right]b \qquad \text{(F-8)}$$

In matrix notation, the problem is

$$\underline{\underline{A}}\,\underline{R} + \underline{\underline{\tilde{C}}}\,\underline{\lambda} = \underline{B} \qquad \text{(F-9a)}$$

$$\underline{\underline{C}}\,\underline{R} - \underline{a} = 0 \qquad \text{(F-9b)}$$

where $\underline{A}$ = coefficient matrix from the integral term

$\underline{C}$ = coefficient matrix generated from the boundary conditions

$\underline{B}$ = vector generated by the second term of the functional

$\underline{a}$ = boundary condition vector

As illustrated in Fig F-2, the additional enforcement of the boundary conditions through the use of Lagrange Multipliers magnifies the scallops. For this reason the two-dimensional problem was solved by enforcing the Neumann conditions through the use of natural boundary conditions.

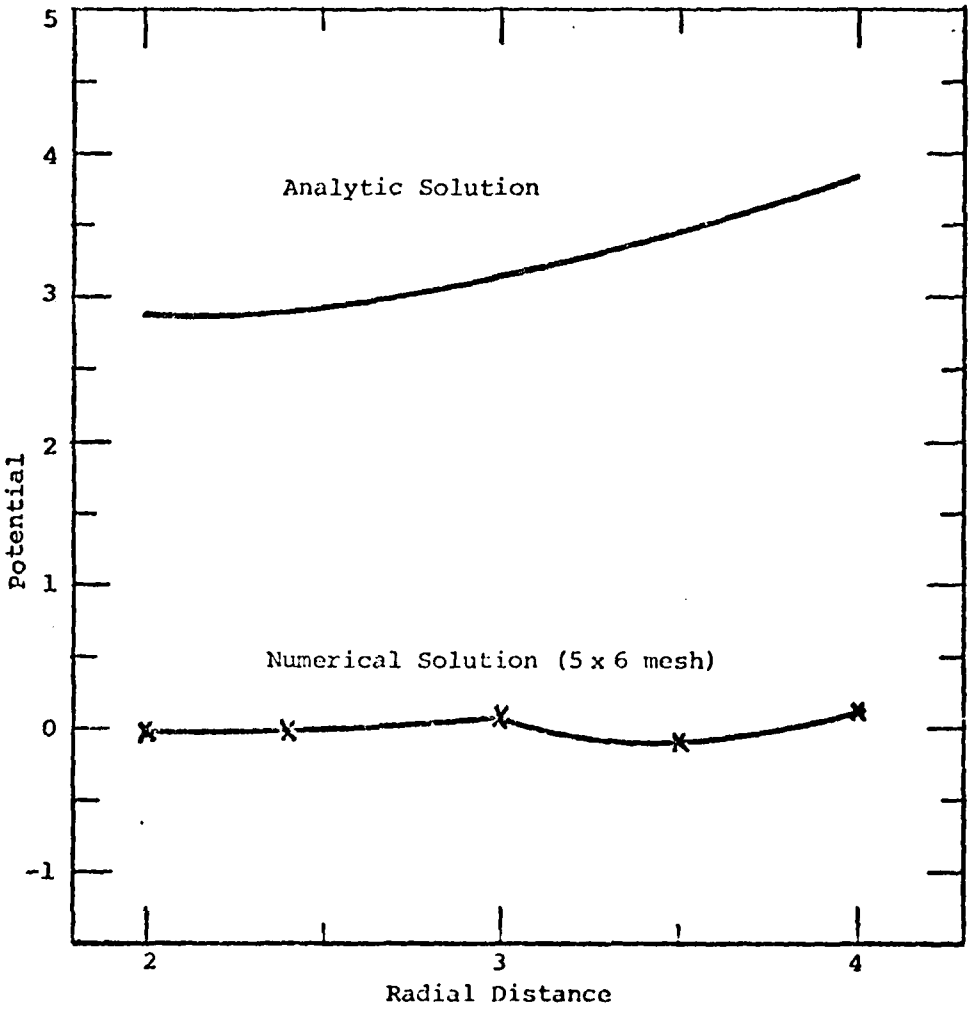


Fig F-1. Potentials along the Line $\theta = 0$ as Solved by Imposing the Boundary Conditions with Lagrange Multipliers and Ignoring the Natural Boundary Conditions.

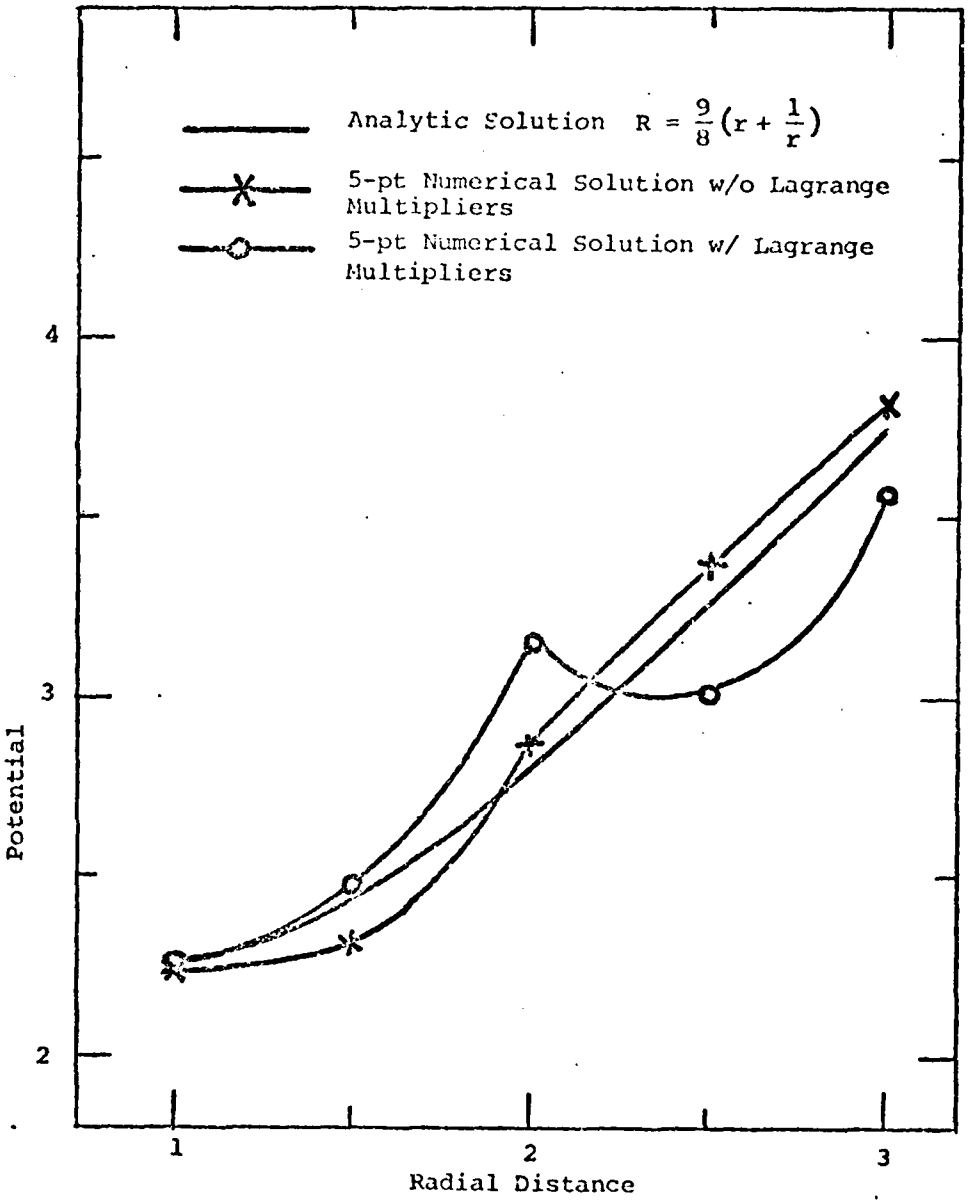


Fig F-2. Solution of the 1-D Problem Using Lagrange Multipliers and Natural Boundary Conditions.

## Appendix G

## Variational Computer Program

The purpose of this appendix is to explain the computer program used to solve the matrix equation generated by the approach using variational calculus. The main program and each subroutine will be explained in a separate sub-section. The format includes an explanation of all variables, references to all equations, and, when necessary, a card-by-card explanation of the program.

### Main Program

The purpose of the main program is to call various subroutines which first set-up and then solve the matrix equation.

Q = Coefficient matrix (stored as a linear array).

Y = Boundary condition vector.

NR = Number of radial mesh points; must be an odd integer.

NA = Number of angular mesh points; must be an even integer.

RI = Inner radius of the cylinder.

RO = Outer radius of the cylinder.

CI = Incoming current density.

H = Radial mesh spacing.

W = Angular mesh spacing.

NQDIAG = Length of the main diagonal of the coefficient matrix. It is the minimum allowable dimension for the Y array.

NQL = Minimum allowable dimension for the Q array.

SIGMA = Conductivity of the cylinder.

Cards 4, 5: LLL is any non-zero integer. Its purpose is to allow for the input of more than one set of data. A card containing a value for LLL must be placed before every card containing input data. The last card in the data deck must be the integer zero. This will stop the program.

Cards 13, 14: The values of the potential are printed out.

Subroutine Data

This subroutine reads in the data and calculates all the parameters required for the solution of the matrix problem.

Card 2: Input data is read in. Free format is used.

Card 5: The length of the Y vector is calculated. This number is the minimum allowable dimension for array Y.

Card 6: Q is a symmetric matrix. The lower triangular of Q is stored in a linear array, the length of which is determined by the given formula. It is the minimum allowable dimension for array Q.

Subroutine QSETUP

This subroutine sets up the coefficient matrix, Q.

Cards 3, 4: The Q array is zeroed.

Card 5: A DO LOOP is initiated for the calculation of the coefficients of the mesh points.

Card 6: A subroutine is called which calculates the appropriate Simpson's Rule coefficient for each mesh point.

Card 7: The radial distance to each mesh point is calculated.

Cards 8, 9: The constant coefficients from Eqns (4-9) and (4-11) are calculated.

Cards 10 - 20: The appropriate subroutine for is called for the mesh point under consideration, depending on whether it lies along the inner radius, the outer radius, or somewhere in between.

Card 22: Since the matrix is singular, the lower left element will be zero after the Choleski decomposition is applied. This card sets that element to zero.

Subroutine SC

This subroutine calculates the Simpson's Rule coefficient for each mesh point.

Cards 2 - 10: Modular arithmetic is used to determine the radial position of each mesh point, and assign a value according to the following pattern: 1,4,2,4,...4,2,4,1.

Card 11: Since a two-dimensional mesh is being used, Simpson's Rule has to be applied in the angular direction also. This card assigns a value of 2 to mesh points along odd radials, and a value of 4 to those lying along even radials.

Card 12: The angular and radial contributions to the Simpson's Rule coefficient are multiplied together.

Subroutine QINNER, QOUTER, QMIDDLE, and QJUNC.

These subroutines calculate the contributions of each mesh point to the Q matrix. Eqns (4-10) and (4-11) are used to generate the equations in the subroutines. The constant term was not included in these subroutines because it was accounted for in the calculation of C1 and C2 in QSETUP. Since linear symmetric storage is being used, it is necessary to convert from a two-dimensional array to a linear array using Q (I,J) = Q(K) = Q(I (I-1)/2 + J).

Subroutine LSETUP

This subroutine performs a Choleski decomposition of the Q matrix. The diagonal elements are calculated using

$$l_{ii} = \sqrt{a_{ii} - \sum_{j=1}^{i-1} l_{ij}^2} \qquad \text{(G-1)}$$

The remaining elements are calculated using

$$l_{ji} = \frac{1}{l_{ii}} \left( a_{ij} - \sum_{k=1}^{i-1} l_{jk} l_{ik} \right) \qquad j > i \qquad \text{(G-2)}$$

Cards 3, 5: A DO LOOP is initialized which spans all but the final element of the lower triangular matrix. This element has been set to zero in the previous subroutine.

Card 6: IB is used to span the elements in the first column of the matrix.

Card 7: JB is used to span the row elements.

Card 8: ID is used to span the main diagonal elements.

Card 9: I1 is a parameter used by VPROD to indicate the number of pairs of elements being multiplied together. It is always one less than the column index of the element being calculated.

Card 10: Eqn (G-1) is used to calculate the main diagonal elements.

Cards 11, 12: A DO LOOP is initialized which spans all elements beneath the main diagonal element just calculated.

Cards 13 - 15: Eqn (G-2) is used to calculate the elements below the main diagonal.

Subroutine YSET

This subroutine calculates the inhomogeneous boundary condition vector. It is the right side of Eqn (4-5). (Its infinite sum representation is shown in Eqn (4-18).) The only non-zero values of this vector will be those corresponding to a mesh point lying on the outer radius.

Cards 3, 4: The Y array is reset to zero.

Card 5: A DO LOOP is initialized wh. spans all mesh points.

Card 6: If the mesh point under consideration does not lie along the outer boundary, the DO LOOP continues without assigning it a value.

Cards 7, 8: The appropriate Simpson's Rule coefficient is determined depending on whether the point lies along an odd or even radial.

Card 9, 10: Eqn (4-18) is used to calculate the boundary value. In this case, $f(\theta) = \cos\theta$.

Card 12: The last value of the vector is arbitrarily set to zero, as explained in the last paragraph on page 14.

Subroutine SOLVE

This subroutine solves the matrix equation $\underline{L}\tilde{\underline{L}}\,\underline{\phi} = \underline{y}$ by first calculating $\underline{x}$ in $\underline{L}\,\underline{x} = \underline{y}$ using forward substitution, and then calculating $\phi$ in $\tilde{\underline{L}}\,\phi = \underline{x}$ using backward substitution.

Card 5: A DO LOOP is initialized which spans all but the lower left element of the matrix.

Card 6: I1 is used with VPROD to indicate the number of pairs of elements being multiplied together.

Card 7: IB is an index which enables VPROD to calculate the row products of $\underline{L}$.

Card 8: ID spans each element of the main diagonal.

Card 9: The values of $\underline{x}$ are calculated and stored in the Y array.

Card 10: The last element of $\underline{x}$ is set to zero.

Card 11: This card initiates the back substitution scheme by calculating the second last element of $\underline{\phi}$ and storing it in the Y array.

Cards 12, 13: Since the last element of the $\underline{\phi}$ vector is zero, and the second last element has just been calculated, the DO LOOP must be indexed to span NQDIAG-2 elements.

Card 14: I is used to index the calculation of the Ith element of $\underline{\phi}$.

Card 16: L spans each element of the main diagonal.

Cards 17 - 19: This loop calculates the column products of $\underline{\underline{\tilde{L}}}$ with the corresponding terms of the $\underline{\phi}$ vector.

Card 20: The terms of the $\underline{\phi}$ vector are computed and stored in the y array.

Cards 21 - 26: The $\underline{\phi}$ vector is normalized as explained in the last paragraph on page 14.

```
      PROGRAM THESIS(INPUT,OUTPUT)
      DIMENSION Q(46000),Y(500)
   41 FORMAT(1X,15F5.4)
   25 READ*,LLL
      IF(LLL.EQ.0)STOP
      CALL DATA(NR,NA,RI,RO,CI,M,N,NODIAG,N,NOL,SIGMA)
      PRINT*," "
      PRINT*,"NA=",NA,"   NP=",NP
      CALL QSETUP(NR,RI,M,N,1,NA,Q,NOL,NODIAG)
      CALL LSETUP(Q,NODIAG)
      CALL YSET(NODIAG,NR,N,NA,Y,RO,M)
      CALL SOLVE(Q,Y,NODIAG,NOL)
      DO 61 I=1,NR
   61 WRITE 30,Y(I)
      GO TO 25
      END
```

```
      SUBROUTINE DATA(NP,NA,RI,RO,CI,M,N,NODIAG,N,NOL,SIGMA)
      READ*,NP,NA,RI,RO,CI,SIGMA
      M=(RO-RI)/FLOAT(NR-1)
      N=6.28318531/10./FLOAT(NA)
      NODIAG=NA*N
      NOL=NODIAG*(NODIAG+1)/2
      RETURN
      END
```

```
      SUBROUTINE QSETUP(NR,RT,H,W,I,MP,Q,NQL,NODIAG)
      DIMENSION Q(1)
      DO 1 L=1,NQL
1     Q(L)=0.
      DO 2 I=1,NODIAG
      CALL SC(I,NR,MOD1,A)
      R=1+MOD1*H
      C1=.25*W*A/H
      C2=.25*H*A/(R*W)/2.
      IF(MOD1.EQ.0)GO TO 3
      IF(MOD1.EQ.NR-1)GO TO 4
      IF(MOD(MOD1,2).EQ.0)GO TO 5
      GO TO 6
3     CALL QINNER(C1,C2,I,Q,NR,NQL,NODIAG)
      GO TO 2
4     CALL QOUTER(C1,C2,I,Q,NR,NQL,NODIAG)
      GO TO 2
5     CALL QJUNC(C1,C2,I,Q,NR,NQL,NODIAG)
      GO TO 2
6     CALL QMIDDLE(C1,C2,I,Q,NR,NQL,NODIAG)
2     CONTINUE
      Q(NQL)=0.
      RETURN
      END
```

```
      SUBROUTINE SC(J,NR,MOD1,A)
      J1=J-1
      NR1=NR-1
      MC1=MOD(J1,NR)
      MOD2=MOD(MOD1,NR1)
      IF(MOD2.EQ.0)GO TO 1
      IF(MOD(MOD2,2).EQ.0)AI=2.
      IF(MOD(MOD2,2).NE.0)AI=4.
      GO TO 2
1     AI=1.
2     MJ=2+2*((J-1)/NR-2*(((I-1)/NR)/2))
      A=AI*FLOAT(MJ)/3.
      RETURN
      END
```

```
      SUBROUTINE CINNER(C1,C2,K,Q,NR,MDL,MODIAG)
      DIMENSION Q(1)
      Q(K*(K-1)/2+K)=Q(K*(K-1)/2+K)+9.*C1
      Q((K+1)*K/2+K)=Q((K+1)*K/2+K)-12.*C1
      Q((K+2)*(K+1)/2+K)=Q((K+2)*(K+1)/2+K)+3.*C1
      Q((K+1)*K/2+K+1)=Q((K+1)*K/2+K+1)+16.*C1
      Q((K+2)*(K+1)/2+K+1)=Q((K+2)*(K+1)/2+K+1)-4.*C1
      Q((K+2)*(K+1)/2+K+2)=Q((K+2)*(K+1)/2+K+2)+1.*C1
      K2=MOD(K+2*NR,MODIAG)
      IF(K2.EQ.0)K2=MODIAG
      K1=MOD(K+NR,MODIAG)
      IF(K1.EQ.0)K1=MODIAG
      Q(K2*(K2-1)/2+K2)=Q(K2*(K2-1)/2+K2)+C2
      IF(K2.LT.K1)Q(K1*(K1-1)/2+K2)=Q(K1*(K1-1)/2+K2)-4.*C2
      IF(K1.LT.K2)Q(K2*(K2-1)/2+K1)=Q(K2*(K2-1)/2+K1)-4.*C2
      IF(K2.LT.K)Q(K*(K-1)/2+K2)=Q(K*(K-1)/2+K2)+3.*C2
      IF(K.LT.K2)Q(K2*(K2-1)/2+K)=Q(K2*(K2-1)/2+K)+3.*C2
      Q(K1*(K1-1)/2+K1)=Q(K1*(K1-1)/2+K1)+16.*C2
      IF(K1.LT.K)Q(K*(K-1)/2+K1)=Q(K*(K-1)/2+K1)-12.*C2
      IF(K.LT.K1)Q(K1*(K1-1)/2+K)=Q(K1*(K1-1)/2+K)-12.*C2
      Q(K*(K-1)/2+K)=Q(K*(K-1)/2+K)+9.*C2
      K2=K-2*NR
      K1=K-NR
      IF(K1.LE.0)K1=K1+MODIAG
      IF(K2.LE.0)K2=K2+MODIAG
      Q(K2*(K2-1)/2+K2)=Q(K2*(K2-1)/2+K2)+C2
      IF(K2.LT.K1)Q(K1*(K1-1)/2+K2)=Q(K1*(K1-1)/2+K2)-4.*C2
      IF(K1.LT.K2)Q(K2*(K2-1)/2+K1)=Q(K2*(K2-1)/2+K1)-4.*C2
      IF(K2.LT.K)Q(K*(K-1)/2+K2)=Q(K*(K-1)/2+K2)+3.*C2
      IF(K.LT.K2)Q(K2*(K2-1)/2+K)=Q(K2*(K2-1)/2+K)+3.*C2
      Q(K1*(K1-1)/2+K1)=Q(K1*(K1-1)/2+K1)+16.*C2
      IF(K1.LT.K)Q(K*(K-1)/2+K1)=Q(K*(K-1)/2+K1)-12.*C2
      IF(K.LT.K1)Q(K1*(K1-1)/2+K)=Q(K1*(K1-1)/2+K)-12.*C2
      Q(K*(K-1)/2+K)=Q(K*(K-1)/2+K)+9.*C2
      RETURN
      END
```

```
SUBROUTINE SOURCE(C1,C2,K,Q,NR,NCL,NSDIAG)
DIMENSION Q(1)
Q((K-2)*(K-3)/2+K-2)=Q((K-2)*(K-3)/2+K-2)+1.*C1
Q((K-1)*(K-2)/2+K-2)=Q((K-1)*(K-2)/2+K-2)-4.*C1
Q(K*(K-1)/2+K-2)=Q(K*(K-1)/2+K-2)+3.*C1
Q((K-1)*(K-2)/2+K-1)=Q((K-1)*(K-2)/2+K-1)+10.*C1
Q(K*(K-1)/2+K-1)=Q(K*(K-1)/2+K-1)-12.*C1
Q(K*(K-1)/2+K)=Q(K*(K-1)/2+K)+9.*C1
K2=MOD(K+2*NR,NSDIAG)
IF(K2.EQ.0)K2=NSDIAG
K1=MOD(K+NR,NSDIAG)
IF(K1.EQ.0)K1=NSDIAG
Q(K2*(K2-1)/2+K2)=Q(K2*(K2-1)/2+K2)+C2
IF(K2.LT.K1)Q(K1*(K1-1)/2+K2)=Q(K1*(K1-1)/2+K2)-4.*C2
IF(K1.LT.K2)Q(K2*(K2-1)/2+K1)=Q(K2*(K2-1)/2+K1)-4.*C2
IF(K2.LT.K)Q(K*(K-1)/2+K2)=Q(K*(K-1)/2+K2)+3.*C2
IF(K.LT.K2)Q(K2*(K2-1)/2+K)=Q(K2*(K2-1)/2+K)+3.*C2
Q(K1*(K1-1)/2+K1)=Q(K1*(K1-1)/2+K1)+10.*C2
IF(K1.LT.K)Q(K*(K-1)/2+K1)=Q(K*(K-1)/2+K1)-12.*C2
IF(K.LT.K1)Q(K1*(K1-1)/2+K)=Q(K1*(K1-1)/2+K)-12.*C2
Q(K*(K-1)/2+K)=Q(K*(K-1)/2+K)+9.*C2
K2=K-2*NR
K1=K-NR
IF(K1.LE.0)K1=K1+NSDIAG
IF(K2.LE.0)K2=K2+NSDIAG
Q(K2*(K2-1)/2+K2)=Q(K2*(K2-1)/2+K2)+C2
IF(K2.LT.K1)Q(K1*(K1-1)/2+K2)=Q(K1*(K1-1)/2+K2)-4.*C2
IF(K1.LT.K2)Q(K2*(K2-1)/2+K1)=Q(K2*(K2-1)/2+K1)-4.*C2
IF(K2.LT.K)Q(K*(K-1)/2+K2)=Q(K*(K-1)/2+K2)+3.*C2
IF(K.LT.K2)Q(K2*(K2-1)/2+K)=Q(K2*(K2-1)/2+K)+3.*C2
Q(K1*(K1-1)/2+K1)=Q(K1*(K1-1)/2+K1)+10.*C2
IF(K1.LT.K)Q(K*(K-1)/2+K1)=Q(K*(K-1)/2+K1)-12.*C2
IF(K.LT.K1)Q(K1*(K1-1)/2+K)=Q(K1*(K1-1)/2+K)-12.*C2
Q(K*(K-1)/2+K)=Q(K*(K-1)/2+K)+9.*C2
RETURN
END
```

```
      SUBROUTINE ONEDGE(C1,C2,K,Q,NR,NOL,NODIAG)
      DIMENSION Q(1)
      Q((K-1)*(K-2)/2+K-1)=Q((K-1)*(K-2)/2+K-1)+1.*C1
      Q((K+1)*K/2+K-1)=Q((K+1)*K/2+K-1)-1.*C1
      Q((K+1)*K/2+K+1)=Q((K+1)*K/2+K+1)+1.*C1
      K2=K-2*NR
      IF(K2.EQ.0)K2=NODIAG
      K1=K-NR
      IF(K1.EQ.0)K1=NODIAG
      Q(K2*(K2-1)/2+K2)=Q(K2*(K2-1)/2+K2)+C2
      IF(K2.LT.K1)Q(K1*(K1-1)/2+K2)=Q(K1*(K1-1)/2+K2)-4.*C2
      IF(K1.LT.K2)Q(K2*(K2-1)/2+K1)=Q(K2*(K2-1)/2+K1)-4.*C2
      IF(K2.LT.K)Q(K*(K-1)/2+K2)=Q(K*(K-1)/2+K2)+3.*C2
      IF(K.LT.K2)Q(K2*(K2-1)/2+K)=Q(K2*(K2-1)/2+K)+3.*C2
      Q(K1*(K1-1)/2+K1)=Q(K1*(K1-1)/2+K1)+16.*C2
      IF(K1.LT.K)Q(K*(K-1)/2+K1)=Q(K*(K-1)/2+K1)-12.*C2
      IF(K.LT.K1)Q(K1*(K1-1)/2+K)=Q(K1*(K1-1)/2+K)-12.*C2
      Q(K*(K-1)/2+K)=Q(K*(K-1)/2+K)+9.*C2
      K2=K-2*NR
      K1=K-NR
      IF(K1.LE.0)K1=K1+NODIAG
      IF(K2.LE.0)K2=K2+NODIAG
      Q(K2*(K2-1)/2+K2)=Q(K2*(K2-1)/2+K2)+C2
      IF(K2.LT.K1)Q(K1*(K1-1)/2+K2)=Q(K1*(K1-1)/2+K2)-4.*C2
      IF(K1.LT.K2)Q(K2*(K2-1)/2+K1)=Q(K2*(K2-1)/2+K1)-4.*C2
      IF(K2.LT.K)Q(K*(K-1)/2+K2)=Q(K*(K-1)/2+K2)+3.*C2
      IF(K.LT.K2)Q(K2*(K2-1)/2+K)=Q(K2*(K2-1)/2+K)+3.*C2
      Q(K1*(K1-1)/2+K1)=Q(K1*(K1-1)/2+K1)+16.*C2
      IF(K1.LT.K)Q(K*(K-1)/2+K1)=Q(K*(K-1)/2+K1)-12.*C2
      IF(K.LT.K1)Q(K1*(K1-1)/2+K)=Q(K1*(K1-1)/2+K)-12.*C2
      Q(K*(K-1)/2+K)=Q(K*(K-1)/2+K)+9.*C2
      RETURN
      END
```

```
      SUBROUTINE OBJNC(C1,C2,K,O,NF,NC,NDIAG)
      DIMENSION O(1)
      O(K*(K-1)/2+K)=O(K*(K-1)/2+K)+4.5*C1
      O((K+1)*K/2+K)=O((K+1)*K/2+K)-6.*C1
      O((K+2)*(K+1)/2+K)=O((K+2)*(K+1)/2+K)+1.5*C1
      O((K+2)*(K+1)/2+K+1)=O((K+2)*(K+1)/2+K+1)-2.*C1
      O((K+1)*K/2+K+1)=O((K+1)*K/2+K+1)+3.*C1
      O((K+2)*(K+1)/2+K+2)=O((K+2)*(K+1)/2+K+2)+.5*C1
      O((K-2)*(K-3)/2+K-2)=O((K-2)*(K-3)/2+K-2)+.5*C1
      O((K-1)*(K-2)/2+K-2)=O((K-1)*(K-2)/2+K-2)-2.*C1
      O(K*(K-1)/2+K-2)=O(K*(K-1)/2+K-2)+1.5*C1
      O((K-1)*(K-2)/2+K-1)=O((K-1)*(K-2)/2+K-1)+3.*C1
      O(K*(K-1)/2+K-1)=O(K*(K-1)/2+K-1)-3.*C1
      O(K*(K-1)/2+K)=O(K*(K-1)/2+K)+4.5*C1
      K2=K-2*NF
      IF(K2.EQ.0)K2=NDIAG
      K1=MOD(K+NF,NDIAG)
      IF(K1.EQ.0)K1=NDIAG
      O(K2*(K2-1)/2+K2)=O(K2*(K2-1)/2+K2)+C2
      IF(K2.LT.K1)O(K1*(K1-1)/2+K2)=O(K1*(K1-1)/2+K2)-4.*C2
      IF(K1.LT.K2)O(K2*(K2-1)/2+K1)=O(K2*(K2-1)/2+K1)-4.*C2
      IF(K2.LT.K)O(K*(K-1)/2+K2)=O(K*(K-1)/2+K2)+3.*C2
      IF(K.LT.K2)O(K2*(K2-1)/2+K)=O(K2*(K2-1)/2+K)+3.*C2
      O(K1*(K1-1)/2+K1)=O(K1*(K1-1)/2+K1)+16.*C2
      IF(K1.LT.K)O(K*(K-1)/2+K1)=O(K*(K-1)/2+K1)-12.*C2
      IF(K.LT.K1)O(K1*(K1-1)/2+K)=O(K1*(K1-1)/2+K)-12.*C2
      O(K*(K-1)/2+K)=O(K*(K-1)/2+K)+9.*C2
      K2=K-2*NF
      K1=K-NF
      IF(K1.LE.0)K1=K1+NDIAG
      IF(K2.LE.0)K2=K2+NDIAG
      O(K2*(K2-1)/2+K2)=O(K2*(K2-1)/2+K2)+C2
      IF(K2.LT.K1)O(K1*(K1-1)/2+K2)=O(K1*(K1-1)/2+K2)-4.*C2
      IF(K1.LT.K2)O(K2*(K2-1)/2+K1)=O(K2*(K2-1)/2+K1)-4.*C2
      IF(K2.LT.K)O(K*(K-1)/2+K2)=O(K*(K-1)/2+K2)+3.*C2
      IF(K.LT.K2)O(K2*(K2-1)/2+K)=O(K2*(K2-1)/2+K)+3.*C2
      O(K1*(K1-1)/2+K1)=O(K1*(K1-1)/2+K1)+16.*C2
      IF(K1.LT.K)O(K*(K-1)/2+K1)=O(K*(K-1)/2+K1)-12.*C2
      IF(K.LT.K1)O(K1*(K1-1)/2+K)=O(K1*(K1-1)/2+K)-12.*C2
      O(K*(K-1)/2+K)=O(K*(K-1)/2+K)+9.*C2
      RETURN
      END
```

```
      SUBROUTINE LSETUP(C,NODIAG)
      DIMENSION C(1)
      NODIAG1=NODIAG-1
      ID=0
      DO 1 I=1,NODIAG1
      IB=ID+1
      JB=IB
      ID=ID+I
      I1=I-1
      C(ID)=SQRT(C(ID)-VPROD(C(IB),1,C(IB),1,I1,V))
      JL=I+1
      DO 1 J=JL,NODIAG
      JB=JB+J-1
      JT=JB+I-1
    1 C(JT)=(C(JT)-VPROD(C(IB),1,C(JB),1,I1,V))/C(ID)
      RETURN
      END
```

```
      SUBROUTINE YSET(NODIAG,NR,N,NA,Y,R),W)
      DIMENSION Y(1)
      DO 1 I=1,NODIAG
    1 Y(I)=0.
      DO 2 I=1,NODIAG
      IF(MCO(I,NR).NE.1)GO TO 2
      IF(MCO(I,2).EQ.1)SIMP=4./3.
      IF(MCO(I,2).NE.0)SIMP=2./3.
      CT=COS((I/N2-1)*(3.2831853071E)/N1)
      Y(I)=CT**2*SIMP*W
    2 CONTINUE
      Y(NODIAG)=1.
      RETURN
      END
```

```
      SUBROUTINE SOLVE(Q,Y,NODIAG,NQL)
      DIMENSION Q(1),Y(1)
      NODIAG1=NODIAG-1
      I0=0
      DO 1 I=1,NODIAG1
      I1=I-1
      IB=I0+1
      I0=I0+I
    1 Y(I)=(Y(I)-VPROD(Q(IB),1,Y(1),1,I1,I))/Q(I0)
      Y(NODIAG)=0.
      Y(NODIAG1)=Y(NODIAG1)/Q(NQL-NODIAG)
      NODIAG2=NODIAG-2
      DO 2 II=1,NODIAG2
      I=NODIAG1-II
      TEMP=0.
      L=NQL-II-NODIAG
      DO 3 K=1,II
      TEMP=TEMP+Q(L)*Y(NODIAG1+1-K)
    3 L=L-NODIAG1+K
    2 Y(I)=(Y(I)-TEMP)/Q(L)
      TEMP=0.
      DO 4 I=1,NODIAG
    4 TEMP=TEMP+Y(I)
      TEMP=TEMP/NODIAG
      DO 5 I=1,NODIAG
    5 Y(I)=Y(I)-TEMP
      RETURN
      END
```

Appendix H

## Derivation of the Green's Function and Iteration Formulas

This appendix contains three derivations. First, the form of the Green's function, $G(\vec{x}-\vec{x}')$ is derived. Secondly, detailed iterative formulas are derived for $\psi(\vec{x})$ and $\phi(\vec{x})$ as used in Eqns (5-8) and (5-9) respectively.

### Derivation of the Green's Function

As stated in Chapter V, if $G(\vec{x}-\vec{x}')$ is a solution to $\nabla^2\phi = 0$, then

$$\nabla^2 G(\vec{x}-\vec{x}') = \delta(\vec{x}-\vec{x}') \tag{H-1}$$

Since the problem is being solved in cylindrical coordinates, the delta function takes the form

$$\delta(\vec{x}-\vec{x}') = \frac{\delta(r)}{\pi r} \tag{H-2}$$

where $r = |\vec{x}-\vec{x}'|$

This equality can easily be seen from the following:

$$\int f(\vec{x})\delta(\vec{x})\,d\vec{x} = f(0) \tag{H-3}$$

where $f(\vec{x})$ is a test function, (Ref: 11, 29).

In terms of an integral over r and $\theta$, the left side of Eqn (H-3) becomes

$$\int_0^{2\pi}\int_0^{\infty} f(r)\,\frac{\delta(r)}{\pi r}\,r\,dr\,d\theta \stackrel{?}{=} f(0) \qquad \text{(H-4)}$$

$$2\int_0^{\infty} f(r)\,\delta(r)\,dr \stackrel{?}{=} f(0) \qquad \text{(H-5)}$$

$$2\left[\frac{1}{2}\,f(0)\right] = f(0) \qquad \text{(H-6)}$$

The equality holds, therefore Eqn (H-2) is valid.

Substituting Eqn (H-2) into Eqn (H-1), and writing $\nabla^2$ in cylindrical coordinates yields

$$\frac{1}{r}\frac{\partial}{\partial r}\left(r\frac{\partial G}{\partial r}\right) + \frac{1}{r^2}\frac{\partial^2 G}{\partial \theta^2} = \frac{\delta(r)}{\pi r} \qquad \text{(H-7)}$$

Assuming the Green's function does not depend on angle, the partial derivative with respect to $\theta$ vanishes. Thus Eqn (H-7) becomes

$$\frac{d}{dr}\left(r\frac{dG}{dr}\right) = \frac{\delta(r)}{\pi} \qquad \text{(H-8)}$$

Integration of Eqn (H-8) yields

$$r\frac{dG}{dr} = \frac{1}{\pi} \qquad \text{(H-9)}$$

Equation (H-9) is easily solved for G:

$$G(\vec{x}-\vec{x}') = \frac{\ln r}{\pi} + H(\vec{x},\vec{x}') \qquad \text{(H-10)}$$

where

$$\nabla^2 H(\vec{x},\vec{x}') = 0$$

and

$$r = |\vec{x} - \vec{x}'|$$

Ref (8, 92-102) contains a detailed discussion of logarithmic potentials, including derivations which amplify on the factor of $1/\pi$.

If $H(\vec{x},\vec{x}')$ is set to zero, the gradient of G is

$$\nabla G(\vec{x} - \vec{x}') = \nabla \frac{\ln r}{\pi} \qquad \text{(H-11)}$$

$$\approx \left(\frac{1}{\pi r}\right) \hat{r} \qquad \text{(H-12)}$$

$$= \frac{\vec{r}}{\pi r^2} \qquad \text{(H-13)}$$

Since the Green's function is symmetric

$$\nabla' G(\vec{x}' - \vec{x}) = \frac{\vec{x}' - \vec{x}}{\pi |\vec{x}' - \vec{x}|^2} \qquad \text{(H-14)}$$

Equations (H-10) and (H-14) are used in conjunction with Eqns (5-8) and (5-9) to solve for $\phi$.

Iterative Formula for $\psi(x)$

The formula for $\psi$ is given in Eqn (5-8) as

$$\psi(\vec{x}) = -\int_S G(\vec{x}' - \vec{x}) \nabla \phi(\vec{x}') \cdot da' \qquad \text{(H-15)}$$

Substituting Eqn (H-10) and performing the dot product operation yields

$$\Psi(\vec{x}) = -\int_S \frac{\ln|\vec{x}'-\vec{x}|}{\pi} \frac{\partial\phi}{\partial r} ds \qquad \text{(H-16)}$$

Since there is only a contribution from the outer boundary, Eqn (H-16) can be simplified to

$$\Psi(\vec{x}) = \frac{-b}{\pi}\int_0^{2\pi} \ln|\vec{x}'-\vec{x}| \frac{\partial\phi}{\partial r} d\theta \qquad \text{(H-17)}$$

Or, as a summation over N mesh points on the outer boundary

$$\Psi(\vec{x}) = \frac{-b\Delta\theta}{\pi}\sum_{n=1}^{N} \ln|\vec{x}'-\vec{x}|_n \frac{\partial\phi}{\partial r}_n \qquad \text{(H-18)}$$

When calculating $\Psi$ on the inner boundary due to the source points on the outer boundary, the above formula presents no problem. However, when calculating $\Psi$ on the outer boundary, the term $|\vec{x}'-\vec{x}|$ approaches zero as $\vec{x}'$ approaches $\vec{x}$. Fortunately this "self-contribution" term can be calculated analytically.

Figure (H-1) illustrates the schematics for the calculation of the "self-contribution" term. The point $\phi_o$ cannot be evaluated numerically. Points $\phi_+$ and $\phi_-$ are neighboring mesh points.

If the points are close together, $\theta'$ is very small, and $\partial\phi/\partial r$ is approximately constant over the interval. So for a small interval,

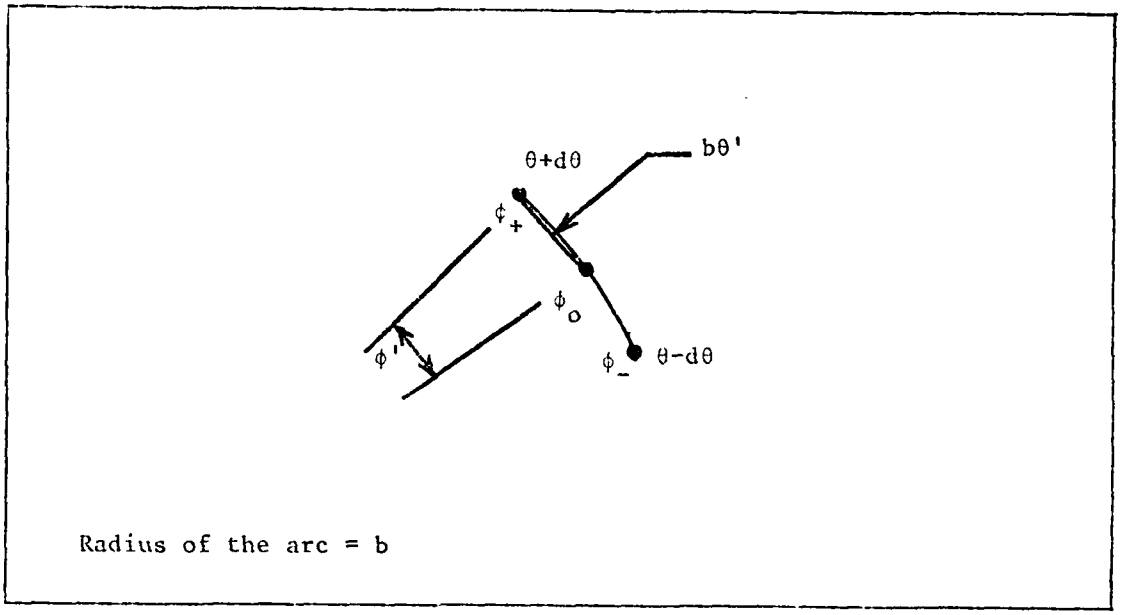


Fig (H-1). Schematic for Calculating the Singular Portion of Eqn (H-17).

Eqn (H-17) can be written

$$\Psi \approx \frac{-1}{\pi} \frac{\partial \phi}{\partial r} \int_{\theta-d\theta}^{\theta+d\theta} b \ln |b\theta'| \, d\theta \qquad \text{(H-19)}$$

With a change of variable, $b\theta' = x$, this equation becomes

$$\Psi \approx \frac{-2}{\pi} \frac{\partial \phi}{\partial r} \int_{0}^{bd\theta} \ln x \, dx \qquad \text{(H-20)}$$

The factor of 2 is needed because the integration is over two segments of length $bd\theta$. Eqn (H-20) evaluates to

$$\Psi \approx \frac{-2}{\pi} \frac{\partial \phi}{\partial r} bd\theta (\ln bd\theta - 1) \qquad \text{(H-21)}$$

This expression must be added to the numerical non-singular summation of Eqn (H-18).

Iterative Formula for $\phi(\vec{x})$

The formula for $\phi(\vec{x})$ is given in Eqn (5-9). If the surface integral over S is factored into integrals over the inner and outer boundaries, the equation can be written as

$$\Phi(\vec{x}) = \Psi(\vec{x}) + \int_a \frac{\phi(\vec{x}')(\vec{x}'-\vec{x})\cdot da}{\pi|\vec{x}'-\vec{x}|^2} + \int_b \frac{\phi(\vec{x}')(\vec{x}'-\vec{x})\cdot da}{\pi|\vec{x}'-\vec{x}|^2} \qquad \text{(H-22)}$$

where Eqn (H-14) has been substituted for $\nabla'G$.

For this derivation, the values of $\phi$ will be evaluated on the inner boundary. Figure H-2 illustrates the method of evaluating the integrals in Eqn (H-22). Consider first the contribution from all points on the inner boundary. Once the dot product operation has been performed, the first integral of Eqn (H-22) can be written as

$$\int_a \frac{\phi(\vec{x}')\hat{n}\cdot(\vec{x}_a'-\vec{x})}{\pi|\vec{x}_a'-\vec{x}|^2}\,ds \qquad \text{(H-23)}$$

As can be seen in Fig H-2, the angle between $\vec{x}_a'-\vec{x}$ and $\hat{n}$ is $-\alpha$. Also since the triangle $0-x_a'-x$ is isosceles, $2\alpha+\theta=\pi$. Thus

$$\hat{n}\cdot(\vec{x}_a'-\vec{x}) = |\vec{x}_a'-\vec{x}|\cos(-\alpha) \qquad \text{(H-24)}$$

$$= -|\vec{x}_a'-\vec{x}|\cos\left(\frac{\pi-\theta}{2}\right) \qquad \text{(H-25)}$$

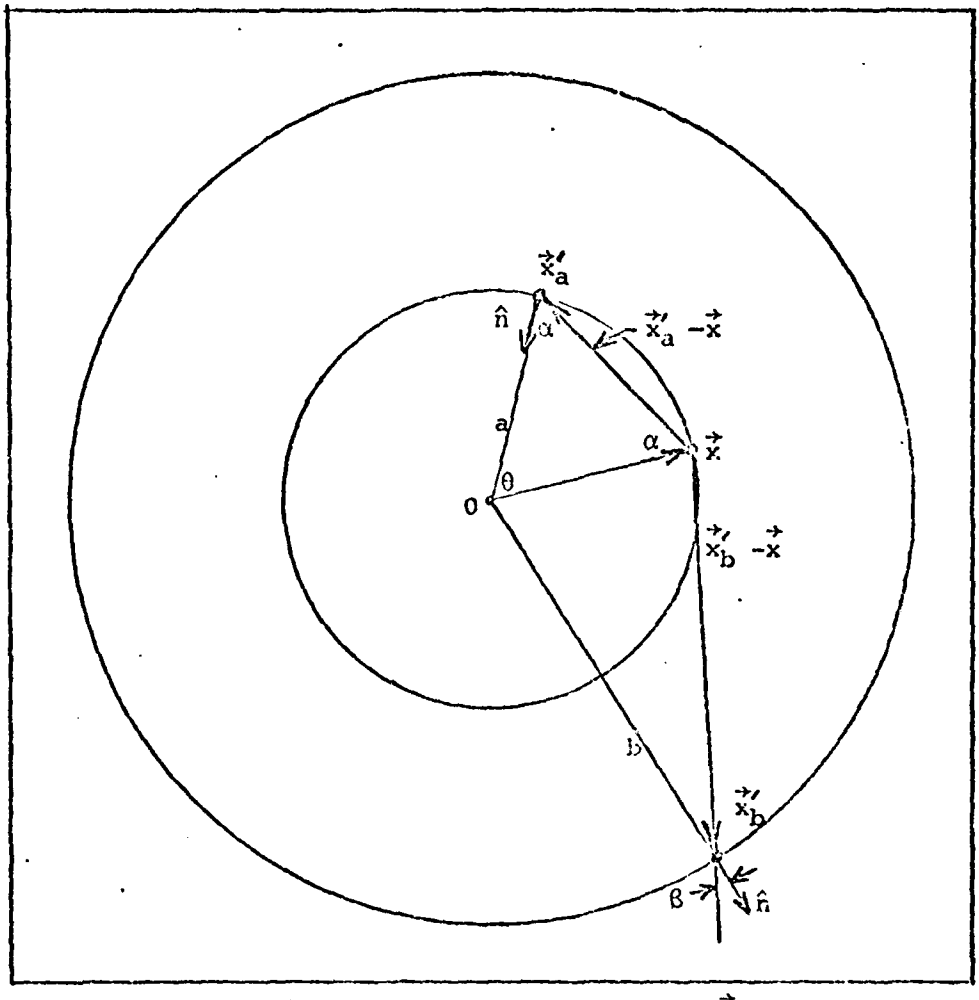


Fig II-2. Schematic Diagram for Calculating $\phi(\vec{x})$ on the Inner Boundary.

$$= -|\vec{x}_a' - \vec{x}| \sin\left(\frac{\theta}{2}\right) \qquad \text{(H-26)}$$

Further, utilizing the Law of Cosines

$$|\vec{x}_a' - \vec{x}|^2 = 2a^2 - 2a^2 \cos\theta \qquad \text{(H-27)}$$

After factoring $2a^2$ and applying a half-angle identity for the sine,

$$|\vec{x}_a' - \vec{x}|^2 = 4a^2 \sin^2\left(\frac{\theta}{2}\right) \qquad \text{(H-28)}$$

When Eqns (H-26) and (H-28) are substituted into Eqn (H-23) the result is

$$\int_a \frac{\phi(\vec{x}')\, \hat{n} \cdot (\vec{x}' - \vec{x})}{\pi |\vec{x}' - \vec{x}|^2}\, ds = \frac{-1}{2a\pi} \int_a \phi(\vec{x}')\, ds \qquad \text{(H-29)}$$

However, as a consequence of the boundary condition

$$\int_{S_{inner}} \frac{\partial \phi}{\partial r}\, ds = 0 \qquad \text{(H-30)}$$

Eqn (H-29) is also zero. Hence it is not necessary to evaluate this term when calculating $\phi$.

Next, the contribution from all points on the outer boundary is determined. The second integral of Eqn (H-22) can be written

$$\int_b \frac{\phi(\vec{x}')\, |\vec{x}_b' - \vec{x}| \cos\beta}{\pi |\vec{x}_b' - \vec{x}|^3}\, ds \qquad \text{(H-31)}$$

where $\beta$ is the angle between $\vec{x}_b' - \vec{x}$ and the outward normal at the source point. The above integral can be written as the following summation,

$$\frac{b\Delta\theta}{\pi} \sum_{n=1}^{N} \frac{\cos\beta_n\, \phi(\theta)_n}{|\vec{x}_b' - \vec{x}|_n} \qquad \text{(H-32)}$$

where $\beta_n$ and $\vec{x}_b' - \vec{x}$ can be determined from the Law of Cosines.

The iteration formula for $\phi(\vec{x})$ on the inner boundary can now be found by substituting Eqn (H-32) into Eqn (H-22).

$$\phi_a(\vec{x}') = \psi_a(\vec{x}) + \frac{b\Delta\theta}{\pi}\sum_{n=1}^{N}\frac{\cos\beta_n\,\phi(\theta)_n}{|\vec{x}_b' - \vec{x}|_n} \qquad \text{(H-33)}$$

A similar formula for calculating $\phi(\vec{x})$ on the outer boundary can be found by following a similar procedure. The formula is

$$\phi_b(\vec{x}) = \psi_b(\vec{x}) + \frac{a\Delta\theta}{\pi}\sum_{n=1}^{N}\frac{\cos\gamma_n\,\phi(\theta)_n}{|\vec{x}_b' - \vec{x}|_n} \qquad \text{(H-34)}$$

where $\gamma$ is the angle between $\vec{x}_b$ and the outward unit normal at the source points.

A computer program using Eqns (H-18), (H-21), (H-33), and (H-34) to iterate values of $\phi$ can be found in Appendix J.

Appendix I

## Derivation of the Integral Equation for $\phi(x)$

This appendix contains a more rigorous derivation of the integral equation for the potential, Eqn (5-7), and its associated Green's function.

Figure I-1 illustrates the domain for this derivation.

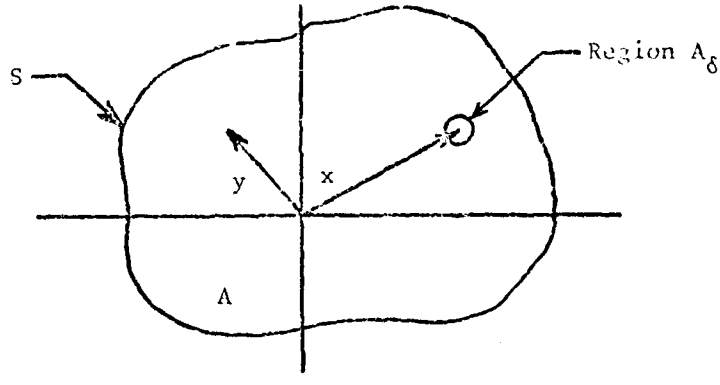


A = Domain of interest
S = Boundary of A
$A_\delta$ = Circle of radius $\delta$ (where $\delta$ is arbitrarily small) centered on point x.
$S_\delta$ = Boundary of $A_\delta$
x,y = Arbitrary vectors
r = y-x

Fig I-1 Domain for the Derivation of the Integral Equation.

The equation for the problem is

$$\nabla^2\phi = 0 \tag{I-1}$$

If $\phi = f(r)$, in cylindrical coordinates Eqn (I-1) is

$$(rf')' = 0 \tag{I-2}$$

which implies

$$f = C \ln r + D \tag{I-3}$$

where C and D are constants of integration. Consider f = ln r. Upon substitution into Eqn (I-1),

$$\nabla^2 f = 0 \qquad r \neq 0 \tag{I-4}$$

Thus, $\nabla^2 f$, like f, is not defined at r = 0. Now, recall Green's second theorem in the form

$$\int_A [\psi \nabla^2 \phi - \phi \nabla^2 \psi] dA = \int_S [\psi \frac{\partial \phi}{\partial n} - \phi \frac{\partial \psi}{\partial n}] ds \tag{I-5}$$

Applying Eqn (I-5) to region $A-A_\delta$ results in

$$\int_{A-A_\delta} [\psi \nabla^2 \phi - \phi \nabla^2 \psi] dA =$$

$$\int_S [\psi \frac{\partial \phi}{\partial n} - \phi \frac{\partial \psi}{\partial n}] ds - \int_{S_\delta} [\psi \frac{\partial \phi}{\partial n} - \phi \frac{\partial \psi}{\partial n}] dS_\delta \tag{I-6}$$

Suppose

$$\psi = \ln |y-x| \tag{I-7}$$

Then, in region $S_\delta$

$$\psi = \ln \delta \tag{I-8}$$

and

$$dS_\delta = \delta d\theta \tag{I-9}$$

So

$$\int_{S_\delta} [\psi \frac{\partial \phi}{\partial n} - \phi \frac{\partial \psi}{\partial n}] dS_\delta = \int_0^{2\pi} [\ln \delta \frac{\partial \phi}{\partial n} - \frac{\phi}{\delta}] \delta d\theta \tag{I-10}$$

AD-A121 727 SPACECRAFT CHARGING(U) AIR FORCE INST OF TECH 2/2
WRIGHT-PATTERSON AFB OH SCHOOL OF ENGINEERING
R A PASSOW DEC 78 AFIT/GNE/PH/78-8

UNCLASSIFIED F/G 22 2 NL

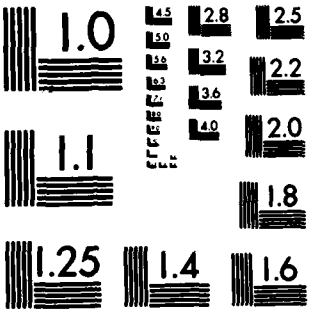

As $\delta$ approaches zero, the integral on the right approaches $-2\pi\phi(x)$, so upon substitution of Eqns (I-7) and (I-10) into Eqn (I-6)

$$\int_A \ln|y-x|\,\nabla^2\phi\,dA = \int_S \left[\ln|y-x|\,\frac{\partial\phi}{\partial n} - \phi\,\frac{\partial}{\partial n}\ln|y-x|\right]ds + 2\pi\phi(x) \quad \text{(I-11)}$$

Or,

$$\phi(x) = \frac{1}{2\pi}\int_A \ln|y-x|\,\nabla^2\phi\,dA - \frac{1}{2\pi}\int_S \left[\ln|y-x|\,\frac{\partial\phi}{\partial n} - \phi\,\frac{\partial}{\partial n}\ln|y-x|\right]ds \quad \text{(I-12)}$$

Since $\nabla^2\phi = 0$,

$$\phi(x) = \frac{1}{2\pi}\int_S \left[\phi(y)\,\frac{\partial}{\partial n}\ln|y-x| - \ln|y-x|\,\frac{\partial\phi}{\partial n}\right]ds \quad \text{(I-13)}$$

Consider a point, $\eta$, on the boundary, S. As x approaches $\eta$

$$\lim_{x\to\eta}\int_S \phi(y)\,\frac{\partial}{\partial n}\ln|y-\eta|\,ds = \pi\phi(\eta) + \int_S \phi(y)\,\frac{\partial}{\partial n}\ln|y-\eta|\,ds \quad \text{(I-14)}$$

Thus, Eqn (I-13) becomes

$$\phi(\eta) = \frac{1}{2}\phi(\eta) + \frac{1}{2\pi}\int_S \phi(y)\,\frac{\partial}{\partial n}\ln|y-\eta|\,ds - \frac{1}{2\pi}\int \ln|y-\eta|\,\frac{\partial\phi}{\partial n}\,ds \quad \text{(I-15)}$$

Note: Eqn (I-14) is derived in Appendix A of Reference 8.

Finally,

$$\phi(r_1) = \frac{1}{\pi}\int_S \phi(y)\frac{\partial}{\partial n}\ln|y-n|\,ds - \frac{1}{\pi}\int_S \ln|y-n|\frac{\partial \phi}{\partial n}\,ds \qquad \text{(I-16)}$$

Eqn (I-16) is valid at the boundary, and if

$$\vec{x} \equiv n \qquad \text{(I-17)}$$

$$\vec{x}' \equiv y \qquad \text{(I-18)}$$

$$G \equiv \ln|\vec{x}'-\vec{x}| \qquad \text{(I-19)}$$

it is seen to be the same as Eqn (5-7).

## Appendix J

### Green's Function Computer Program

This program is divided into seven main parts by groups of three comment cards. Basically, the program follows the iteration scheme outlined in Chapter V.

Part 1: Input data is read in and all required constants are calculated.

Part 2: The value of $\psi$ on the inner and boundaries is calculated as given in Eqns (II-18) and (II-21).

Part 3: Eqn (II-33) is used to calculate $\phi$ at each inner boundary mesh point.

Part 4: Eqn (II-34) is used to calculate $\phi$ at each outer boundary mesh point.

Part 5: All values of $\phi$ are tested for convergence.

Part 6: Eqn (5-14) is used to calculate $\phi$ in Region II.

Part 7: The boundary conditions are calculated as given in Eqn (2-21).

```
      PROGRAM GREEN(INPUT,OUTPUT)
      DIMENSION SA(200),SB(200),PA(200),PB(200),
     1     PASAVE(200),PBSAVE(200)
      READ*,A,B,CI,SIGMA,NA
      SS=A*A+B*B
      ST=2.*A*B
      SBS=2.*B*B
      SAS=2.*A*A
      BS=B*B
      AS=A*A
      PI=3.1415926535
      DA=2.*PI/NA
C
C
C     CALCULATE PSI ON INNER AND OUTER BOUNDARIES.
      DO 1 I=1,NA
      SB(I)=0.
      SA(I)=0.
      DO 3 J=1,NA
      SIMP=(4.-2.*MOD(J+I,2))/3.
      THETA=(I-J)*DA
      SA(I)=SA(I)+SIMP*BND(J,DA,CI,SIGMA)*
     1     ALOG(SQRT(SS-ST*COS(THETA)))
      IF(I.EQ.J)GO TO 3
      IF(MOD(I+J,2).EQ.0)SIMP=4./3.
      IF(MOD(I+J,2).NE.0)SIMP=2./3.
      IF(IABS(MOD(I,NA)-MOD(J,NA)).EQ.1.OR.
     1     IABS(MOD(I,NA)-MOD(J,NA))
     2     .EQ.NA-1)SIMP=1./3.
      SB(I)=SB(I)+SIMP*BND(J,DA,CI,SIGMA)*
     1     ALOG(SQRT(SBS-SAS*COS(THETA)))
    3 CONTINUE
      SB(I)=-B*DA/PI*SB(I)
      SA(I)=-B*DA/PI*SA(I)
      SB(I)=SB(I)-2.*BND(I,DA,CI,SIGMA)/PI*
     1     B*DA*(ALOG(B*DA)-1)
    1 CONTINUE
      DO 4 I=1,NA
      PASAVE(I)=SA(I)
      PBSAVE(I)=SB(I)
      PA(I)=SA(I)
    4 PB(I)=SB(I)
```

```
C
C
C       CALCULATE PHI ON INNER BOUNDARY.
    2   DO 5 I=1,NA
        TEMPB=0.
        DO 6 J=1,NA
        SIMP=(4.,-2.**MOD(J+I,2))/3.
        THETA=(I-J)*DA
        XS=SS-ST*COS(THETA)
        COSA=(XS+BS-AS)/(2.*B*SQRT(XS))
        TEMPB=TEMPB+SIMP*COSA*PB(J)/SQRT(XS)
    6   CONTINUE
        PA(I)=SA(I)+B*DA/PI*TEMPB
    5   CONTINUE
C
C
C       CALCULATE PHI ON OUTER BOUNDARY.
        DO 10 I=1,NA
        TEMPA=0.
        DO 11 J=1,NA
        SIMP=(4.,-2.**MOD(J+I,2))/3.
        THETA=(I-J)*DA
        XS=SS-ST*COS(THETA)
        COSB=(XS+AS-BS)/(2.*A*SQRT(XS))
        COSG=COS(PI-ACOS(COSB))
        TEMPA=TEMPA+SIMP*COSG*PA(J)/SQRT(XS)
   11   CONTINUE
        PB(I)=SB(I)+A*DA/PI*TEMPA
   10   CONTINUE
```

```
C
C
C       TEST FOR CONVERGENCE.
        DO 20 I=1,NA
        TESTA=ABS(PA(I)-PASAVE(I))
        TESTB=ABS(PB(I)-PBSAVE(I))
        IF(TESTA.GT..0001)GO TO 21
   20   IF(TESTB.GT..0001)GO TO 21
        GO TO 22
   21   DO 23 I=1,NA
        PASAVE(I)=PA(I)
   23   PBSAVE(I)=PB(I)
        PRINT*,"ONE ITERATION"
        GO TO 2
   22   DO 24 I=1,NA
   24   PRINT*,PA(I),PB(I),"    NA=",NA
C
C
C       CALCULATE PHI IN REGION II.
        READ*,RP
        DO 31 J=1,NA
        THETAP=(J-1)*360./NA
        TEMP=0
        DO 30 I=1,NA
        THETA=(I-1)*360./NA
        TTP=(THETAP-THETA)*2.*PI/360.
        RRPS=RP*RP+A*A-2.*RP*A*COS(TTP)
        COSG=(RRPS+AS-RP*RP)/(2.*A*SQRT(RRPS))
   30   TEMP=TEMP+COSG*PB(I)/SQRT(RRPS)
        TEMP=TEMP*A*DA/PI
   31   PRINT*,RP,THETAP,TEMP
        END



        FUNCTION BND(J,DA,CI,SIGMA)
        CT=COS((J-1)*DA)
        IF(CT.LT.0.)CT=0.
        BND=CI/SIGMA*(CT-.318309886184)
        RETURN
        END
```

# VITA

Richard Alan Passow was born in Milwaukee, Wisconsin on 19 June 1950. He is the son of Richard R. Passow and Gladys R. Passow. He graduated from Wisconsin Lutheran High School in 1968. In 1973, he graduated with honors from the University of Wisconsin-Milwaukee, receiving a Bachelor of Science Degree in Energy Conversion Engineering as well as a regular commission in the US Army. His initial military schooling consisted of the Air Defense Artillery Basic Course at Fort Bliss, Texas, and Airborne School at Fort Benning, Georgia. Upon completion of this initial training he was assigned to the 2nd Bn 28th Field Artillery in Ansbach, Germany. He served with the unit for three years as Battalion Air Defense Officer and Battalion S-2. Captain Passow then entered the Air Force Institute of Technology in June, 1977.

Permanent address: 5725 N. 67th Street
Milwaukee, WI 53218

UNCLASSIFIED

SECURITY CLASSIFICATION OF THIS PAGE (When Data Entered)

| REPORT DOCUMENTATION PAGE | READ INSTRUCTIONS BEFORE COMPLETING FORM |
|---|---|
| 1. REPORT NUMBER: AFIT/GNE/PH/78-8 | 2. GOVT ACCESSION NO: AD-A112727 |
| 3. RECIPIENT'S CATALOG NUMBER | |
| 4. TITLE (and Subtitle): SPACECRAFT CHARGING | 5. TYPE OF REPORT & PERIOD COVERED: MS Thesis |
| | 6. PERFORMING ORG. REPORT NUMBER |
| 7. AUTHOR(s): Richard A. Passow | 8. CONTRACT OR GRANT NUMBER(s) |
| 9. PERFORMING ORGANIZATION NAME AND ADDRESS: Air Force Institute of Technology (AFIT-EN) Wright-Patterson AFB, Ohio 45433 | 10. PROGRAM ELEMENT, PROJECT, TASK AREA & WORK UNIT NUMBERS |
| 11. CONTROLLING OFFICE NAME AND ADDRESS: CPT Ken A. Dreyer, Air Force Weapons Laboratory, Advanced Concepts Branch, Kirtland AFB, NM 87117 | 12. REPORT DATE: December 1978 |
| | 13. NUMBER OF PAGES: 104 |
| 14. MONITORING AGENCY NAME & ADDRESS (if different from Controlling Office) | 15. SECURITY CLASS. (of this report): Unclassified |
| | 15a. DECLASSIFICATION DOWNGRADING SCHEDULE |

16. DISTRIBUTION STATEMENT (of this Report)

Approved for public release; distribution unlimited

17. DISTRIBUTION STATEMENT (of the abstract entered in Block 20, if different from Report)

18. SUPPLEMENTARY NOTES: Approved for public release IAW AFR 190-17

JOSEPH P. HIPPS, Major, USAF
Director of Information

19. KEY WORDS (Continue on reverse side if necessary and identify by block number)

Charging
Functional
Green's Function
Spacecraft
Variational Calculus

20. ABSTRACT (Continue on reverse side if necessary and identify by block number)

If a spacecraft is exposed to a steady stream of current density, the charge of which is deposited on the surface of a cylindrical, conducting spacecraft, internal electromagnetic fields are generated. If the internal fields are of sufficient strength, undesirable electronic noise or damage may result. This thesis presents three approaches for calculating the induced E-Field: Separation of variables, variational calculus, and the use of Green's functions.

DD FORM 1 JAN 73 1473 EDITION OF 1 NOV 65 IS OBSOLETE

UNCLASSIFIED

SECURITY CLASSIFICATION OF THIS PAGE (When Data Entered)

The spacecraft is modeled as a hollow, infinite cylinder. The fields are calculated for the case in which the incoming current is incident perpendicularly to the longitudinal axis of the cylinder. Basic electro-static theory reveals that the governing equation for the potential is Laplace's Equation, subject to Neumann boundary conditions. This equation is first solved by separation of variables. The $\vec{E}$-Field predicted for representive values of incoming current density are on the order of $10^{-7}$ volts/meter.

Several pitfalls encountered with the variational approach are explained. These include the importance of natural boundary conditions, ensuring continuity of the first derivative across all mesh points, and difficulties encountered in trying to reduce the size of the matrix through "decoupling". The results of this section show that the variational method tends to approximate the analytic solution as the mesh becomes finer.

The Green's function approximations of the potential distribution were consistent with analytic results to at least two significant figures.